1 **Geophysical validation and long-term consistency between**

2 **GOME-2/MetOp-A total ozone column and measurements**

3 **from the sensors GOME/ERS-2, SCIAMACHY/ENVISAT**

4 **and OMI/Aura.**

5

6

7 M. E. Koukouli[1*], D. S. Balis[1],

8 D. Loyola[2], P. Valks[2], W. Zimmer[2], N. Hao[2],

9 J-C. Lambert[3], M. Van Roozendael[3], C. Lerot[3]

10 and R. J. D. Spurr[4].

11

12

13

14

15 1. Laboratory of Atmospheric Physics, Aristotle University of Thessaloniki,

16 Thessaloniki, Greece.

17 2. Deutsches Zentrum für Luft- und Raumfahrt (DLR), Institut für Methodik der

18 Fernerkundung (IMF), 82234 Oberpfaffenhofen, Germany.

19 3. Belgian Institute for Space Aeronomy (BIRA-IASB), 3, Avenue Circulaire, B-1180

20 Brussels, Belgium.

21 4. RT-Solutions, Inc., Cambridge, MA, United States.

22

23

24

25

26

27

28

29

30

31 *Corresponding author: mariliza@auth.gr

32

33

Abstract. The main aim of the paper is to assess the consistency of five years of Global Ozone Monitoring Experiment-2/Metop-A [GOME-2] total ozone columns and the long-term total ozone satellite monitoring database already in existence through an extensive inter-comparison and validation exercise using as reference Brewer and Dobson ground-based measurements. The behaviour of the GOME-2 measurements is being weighed against that of GOME (1995-2011), Ozone Monitoring Experiment [OMI] (since 2004) and the Scanning Imaging Absorption spectroMeter for Atmospheric CartograpHY [SCIAMACHY] (since 2002) total ozone column products. Over the background truth of the ground-based measurements, the total ozone columns are inter-evaluated using a suite of established validation techniques; the GOME-2 time series follow the same patterns as those observed by the other satellite sensors and in particular, on the average, GOME-2 data underestimate GOME data by about 0.80%, and underestimate SCIAMACHY data by 0.37% with no seasonal dependence of the differences between GOME-2, GOME and SCIAMACHY. The latter is expected since the three data sets are based on similar DOAS algorithms. This underestimation of GOME-2 is within the uncertainty of the reference data used in the comparisons. Compared to the OMI sensor, on the average GOME-2 data underestimate OMI_DOAS (collection 3) data by 1.28%, without any significant seasonal dependence of the differences between them. The lack of seasonality might be expected since both the GOME Data Processor [GDP] 4.4 and OMI_DOAS are DOAS-type algorithms and both consider the variability of the stratospheric temperatures in their retrievals. Compared to the OMI_TOMS (collection 3) data, no bias was found. We hence conclude that the GOME-2 total ozone columns are well suitable to continue the long-term global total ozone record with the accuracy needed for climate monitoring studies.

1 Introduction

With the launch of Metop-A on October 19th 2006, a polar orbiting satellite carrying both environmental and meteorological instruments, a new global total ozone data record was started with the GOME-2 instrument. In *Loyola et al.,* 2011, the GOME

68   Data Processor (GDP) version 4.4 retrieval algorithm for GOME-2 total ozone, as

69   well as the first global validation results for three years (2007-2009) using Brewer and

70   Dobson   ground-based   measurements,   were   described.   Several   algorithm

71   improvements were introduced in GDP 4.4 compared to previous versions [*van*

72   *Roozendael et al.,* 2006] such as the improved cloud retrieval algorithms including the

73   discrimination of sun-glint effects, the enhanced treatment for ice and snow

74   conditions, the intra-cloud ozone correction, the updated radiative transfer modelling

75   for large viewing angle conditions and the empirical correction to eliminate a scan

76   angle dependency caused by an unknown bias. To be precise, the forward-scan west-

77   east dependency of more than +1.5% in the previous GDP 4.x data has been largely

78   eliminated in the GDP 4.4 record. The GDP 4.4 algorithm is able enough to deliver

79   real-time data for operational needs while being truly robust in performance. As far as

80   the validation was concerned, for middle latitude comparisons, it has already been

81   shown that the reprocessed GOME-2 GDP 4.4 dataset under-estimates ground-based

82   Dobson ozone by 0.5% in the Northern Hemisphere whereas it over-estimates in the

83   Southern Hemisphere by the same amount. For northern high latitude comparisons, a

84   good comparison relative to the Dobson measurement is found while for the southern

85   high latitude comparisons, an under-estimation of less than 1% is observed. For the

86   tropical stations GOME-2 under-estimates on average by 0 to 2% against the Dobson

87   network. The GOME-2 versus Brewer comparisons over the Northern Hemisphere

88   follow closely the GOME-2 vs. Dobson comparisons and illustrate an underestimation

89   of 1% which tends to be slightly higher (1-2%) over the Arctic.

90

91   Equally important to the stand-alone validation and quality assurance of new

92   atmospheric composition products is to ensure the continuity in the record between

93   current and past missions. Even though the processors analysing the atmospheric

94   signal might be the same, even slight differences in spectral and spatial resolution,

95   detector technology, swath width, and other characteristics, might bring notable

96   differences between the resulting total ozone products from different sensors. In the

97   following, we will delve into the comparisons between GOME-2 total ozone for the

98   years 2007 to 2010 against other three satellite instruments active during these time

99   period, using as reference a background of ground-based total ozone measurements.

100   In Section 2 we discuss the different datasets used with some details on both

101   instruments and algorithms given as well as known issues with the total ozone

102 records, as these were recorded in literature. In Section 3 we show the results and
103 their discussion with the summary and conclusions given in Section 4.
104
105
106 **2   Data Sets and methodology.**
107
108
109 **2.1   The Four Satellite Instruments**
110
111 A very brief description of the four different instruments and the relevant algorithms
112 is given in this following section. For quick reference to the information, the main
113 features of the four instruments, satellite platforms and data versions used in this
114 study are further summarized in Table 1.
115
116 2.1.1   **GOME on board ERS-2**
117
118 The Global Ozone Monitoring Experiment, (GOME), is an across-track nadir-viewing
119 spectrometer on board ERS-2 which is a Sun-synchronous polar orbiting satellite with
120 a period of about 100 min and a local equator crossing time of 10.30h. In normal
121 viewing mode, GOME performs three forward scans followed by a backward scan.
122 Each forward scan has a footprint size of 320 km × 40 km for a 1.5-s detector readout
123 integration time. The maximum swath is 960 km, with nominal scan angle ±31° at the
124 spacecraft, global coverage is achieved at the equator within three days. GOME has
125 3584 spectral channels distributed over four serial readout detectors; the wavelength
126 range is 240 to 793 nm, with a moderate spectral resolution of 0.2 to 0.4 nm. More
127 details on the GOME instrument are given by *Burrows et al.*, 1999a. The instrument
128 was switched off on July 5th, 2011 when the ERS-2 satellite was decommissioned.
129 The GOME total ozone columns presented in this work here are the operational GDP
130 4.1 products [*Van Roozendael et al,* 2006]. Known issues with the GOME total ozone
131 columns reported in [*Balis et al.,* 2007a] include a small mean seasonal dependence
132 remaining north of 40°N and south of 40°S. The amplitude of this seasonality does
133 not exceed 1%−1.5% for the Dobson comparisons and is even less for the Brewer
134 comparisons. Also, there is an overestimation of GOME for SZA between 60° and

135 70°, and a reversal of the SZA trend at 75° for the GDP 4.1/Dobson comparisons. The

136 total column products do not suffer from any long-term drift of quality from 1995 to

137 2003, despite instrument degradation; the stability of the GDP 4.1 ozone data record

138 enables it to be used confidently for ozone trend monitoring.

139

140 2.1.2 **SCIAMACHY on board ENVISAT**

141

142 The Scanning Imaging Absorption spectroMeter for Atmospheric CartograpHY

143 (SCIAMACHY) was launched in March 2002 aboard the European platform

144 ENVISAT and has been operational for more than ten years providing global

145 coverage in approximately six days [*Bovensmann et al.*, 1999]. ENVISAT is in a Sun-

146 synchronous orbit with an inclination of 98.5°, a mean altitude of 796 km and has a

147 period of 100 min, performing about 14 to 15 orbits per day. SCIAMACHY is an

148 eight-channel spectrometer covering the spectral range from 240 nm to 2380 nm and

149 uses different viewing geometries for retrieving total trace gas columns (nadir) and

150 profiles (limb and solar/lunar occultation). The nominal swath is 960 km with a

151 typical footprint size of 60 km x 30 km for ozone observations, global coverage is

152 achieved at the equator within six days. The total ozone column data used in this

153 study are from the SCIAMACHY Differential Optical Absorption Spectroscopy

154 (SDOAS) algorithm, which is the prototype algorithm for GOME(-2) and

155 SCIAMACHY operational products GDP4.x and SGP5.0, with details found in *Lerot*

156 *et al.*, 2009. With respect to ground-based data on the whole, there is no appreciable

157 systematic bias and more than 75% of the measurements used in this paper agree

158 within 5% for the set of ground stations used in *Lerot et al.*, 2009. It is also important

159 to note that the SCIAMACHY total O_3 columns suffer from a small but statistically

160 significant decreasing trend, ranging between from between −0.20 and −0.50% per

161 annum. The issue is related to the well-known degradation effect in SCIAMACHY

162 which generates time-dependent spectral features in the measured reflectances and

163 introduces an artefact trend in the ozone total columns.

164 2.1.3 **OMI on board Aura**

165

166 The Ozone Monitoring Instrument (OMI) [*Levelt et al.,* 2006] is one of four
167 instruments aboard the NASA EOS-Aura satellite, launched on 15 July 2004
168 [*Schoeberl et al.*, 2006]. OMI is a compact nadir viewing, wide swath (daily global
169 coverage), ultraviolet-visible (270 nm to 500 nm) imaging spectrometer that was
170 contributed to the Aura mission by Netherlands and Finland. The foot pixel size at
171 nadir is 13 km x 25 km. In contrast to GOME and SCIMACHY, the foot pixel size is
172 not constant but increases for the off-nadir positions. Two total ozone column data
173 products are available: the OMI-TOMS data product which is based on the long-
174 standing TOMS V8 retrieval algorithm [*Bhartia et al.,* 2004] and the OMI-DOAS
175 data product which is a DOAS type algorithm [*Veefkind et al.,* 2006] developed by the
176 Royal Netherlands Meteorological Institute (KNMI). *Balis et al.,* 2007b, have shown
177 that, although both algorithms infer total ozone column data for OMI ground pixels,
178 they differ in many aspects of their algorithmic approach and this is reflected in the
179 validation and comparison campaigns. *Balis et al., 2007b*, showed a globally averaged
180 agreement of better than 1% for OMI-TOMS data and better than 2% for OMI-DOAS
181 data with the ground-based observations. The OMI-TOMS data product was found to
182 be of high overall quality with no significant dependence on solar zenith angle or
183 latitude. The OMI-DOAS data product had no significant dependence on latitude
184 except for the high latitudes of the Southern Hemisphere where it systematically
185 overestimated the total ozone value. In addition a significant dependence on solar
186 zenith angle is found between OMI-DOAS and ground-based data. In this work, both
187 products will be considered and were extracted from the Aura Validation Data Centre
188 [http://avdc.gsfc.nasa.gov/]. The OMI_TOMS and OMI_DOAS level-2 total ozone
189 data are based on collection 3 level 1b data and have been processed with TOMS v8.5
190 and   OMDOAO3 v1.0.1 algorithms   respectively   (see   ATBD   documents   at
191 http://toms.gsfc.nasa.gov   and   http://www.temis.nl). The well-known "OMI row
192 anomaly" issue, which affects particular viewing directions which correspond to rows
193 on the CCD detector, has been dealt with by discarding observations with the
194 equivalent   quality   flag   as   discussed   in   detail   at
195 http://www.knmi.nl/omi/research/product/index.php.

196 2.1.4 **GOME-2 on board MetOp-A**

197

198   The Global Ozone Monitoring Experiment-2 (GOME-2) instrument is mounted on the

199   flight-direction side of the MetOp-A satellite. GOME-2 is a nadir-viewing scanning

200   spectrometer, with an across-track scan time of 6 seconds and a swath width of 1920

201   km. Global coverage of the sunlit part of the atmosphere can be achieved almost

202   within one day. GOME-2 ground pixels have a footprint size of 80 km x 40 km, four

203   times smaller than those for GOME (320 km x 40 km), and also improved

204   polarisation monitoring and calibration capabilities [*Munro et al.*, 2006]. In the

205   framework of EUMETSAT's Satellite Application Facility on Ozone and

206   Atmospheric Chemistry Monitoring (O3M-SAF), GOME-2 total ozone data are

207   processed at DLR operationally, both in near real time and offline, using the GDP 4.x

208   algorithm [*Valks et al.*, 2011]. However, operational data were based on different

209   versions of level 1b data, and in addition, the satellite measurements showed a scan

210   angle dependency. In order to provide a homogeneous data set the complete GOME-2

211   dataset was reprocessed with GDP 4.4 at the end of 2009 using the most recent level

212   1b data (version 4), plus an additional empirical correction for the east-west scan

213   dependencies as described in *Loyola et al.*, 2011. Refer to this paper for further details

214   on the algorithm and the validation of the total ozone column against ground-based

215   instruments.

216   Within the framework of the O3M-SAF project, the Laboratory of Atmospheric

217   Physics (LAP) at Aristotle University of Thessaloniki, in collaboration with the

218   Hellenic National Meteorological Service, has developed a total ozone validation

219   facility for GOME-2 data, be found at http://lap.physics.auth.gr/eumetsat/totalozone.

220   **2.2   The ground based measurements**

221   Archived total ozone column measurements from the WMO/GAW network that are

222   routinely deposited at the WOUDC in Toronto, Canada (http://www.woudc.org) were

223   used as ground reference. The WOUDC archive contains total ozone column data

224   mainly from Dobson and Brewer UV spectrophotometers and from M-124 UV filter

225   radiometers. A well maintained and calibrated Dobson spectrophotometer measures

226   the ozone column with an estimated accuracy of 1% for direct Sun observations and

227   2–3% for zenith sky or zenith cloud observations for Sun elevation higher than 15°.

228   The Dobson spectrophotometer is a large and manually controlled two-beam

229   instrument based on the differential absorption method in the ultraviolet Huggins

band where ozone exhibits strong absorption features. The measurement principle relies on the ratio of the direct sunlight intensities at two standard wavelengths. Since 1957, Dobson spectrophotometers have been deployed operationally in a worldwide network. The Brewer grating spectrophotometer is in principle similar to the Dobson, however, it has an improved optical design and is fully automated. The ozone column abundance is determined from a combination of four wavelengths between 306 nm and 320 nm. Since the 1980s, Brewer instruments are part of the ground-based networks as well. Most Brewers are single monochromators, but a small number of systems are double monochromators with improved stray light performance.

The WOUDC stations considered and the reasoning behind the particular selection of stations have already been presented in a series of validation papers, such as for the validation of ten years of GOME observations [*Balis et al, 2007a*], the OMI-TOMS and OMI-DOAS dataset [*Balis et al, 2007b*], a new version of the OMI-TOMS algorithm [*Antón et al.,* 2010] and the GOME-2 validation [*Loyola et al., 2011*].

The selection investigation and criteria have been discussed in detail in both Balis et al., 2007a and 2007b. We offer here a brief summary for completion purposes. For each ground-based station a series of statistics and plots were performed, separately for direct sun measurements and zenith-sky observations. Daily coincidences with the satellite central latitude and longitude of the footprint falling within a 150km radius of the ground station were found and used for the creation of monthly, seasonal and yearly time series and scatter plots. Since the WOUDC data are daily means, there is no temporal treatment of the satellite observations. The percentage of the relative differences between ground and satellite TOC is used as the comparative tool for the validation. The statistics are then performed on a per latitude belt basis, per Hemisphere basis and per the totality of the data basis, always keeping the two types of ground-based instruments separate and using only direct sun observations, as the most reliable. In the following, per Hemisphere and per the totality of the data comparisons will be shown and discussed upon, for space reasons.

3   Results and Discussion

In the following section, the long term performance of GOME-2 total ozone columns will firstly be examined against that of the three instruments discussed above over the

262   background of the Dobson and Brewer total ozone columns. In order to compare

263   possible trends, features and regions of special interest, contour representations of the

264   latitudinal variability of the differences against time are presented first. This will

265   enable the pictorial identification of regions and times where each of the instruments

266   might have faced issues, as well as the long term stability of all total ozone column

267   records. Secondly, the time series of the differences averaged over the Northern

268   Hemisphere enables the study of the seasonality effects and possible trends. Thirdly, a

269   contour representation of the differences as a function of SZA and season permits the

270   identification of lingering SZA and seasonal dependencies and how these compare

271   among the different algorithms and instruments.

272   A point to be made at this point is a possible source for the differences between the

273   Dobson and the Brewer comparisons shown later on in this paper. There exists an

274   inherent deviation between the treatment of the ground-based measurements and the

275   analysis of the satellite observations and that is the choice of ozone absorption cross-

276   sections; the ground-based data are analysed using the Bass & Paur, 1985, ozone

277   cross-sections whereas with the GDP 4.x family of algorithms, cross-sections

278   measured with each instrument are used, namely the GOME measured flight model

279   cross sections for O_3, known as the GOME FM98 data [Burrows et al., 1999b] for the

280   GOME and GOME-2 instruments and the SCIAMACHY flight model data (SFM)

281   (Bogumil et al., 2003) for the SCIAMACHY instrument. The exception being TOMS

282   V8 which uses, to the best of our knowledge, the Bass & Paur, 1985, cross-sections. It

283   certainly falls within the plans for the next generation of algorithms, namely the

284   GDP5.0 Direct Fitting algorithm, to harmonise the use of cross-sections for the

285   satellite observations, however this will come at a later stage. On the impact of the

286   temperature, the point as we understand it is more whether some of the reported

287   differences could come from the fact that ground-based data sets use cross-sections at

288   a fixed temperature (while temperature dependences are accounted for in satellite

289   algorithms). We postulate that the answer is most probably yes, and it probably

290   explains part of the different behaviour between Dobson and Brewer instruments as

291   the Dobson measurements are more sensitive to temperature variations.

292

293

3.1 Long term stability

3.1.1 Latitudinal behaviour

In Figure 1 a contour representation of the difference between each of the four satellite instruments and the Dobson total ozone columns is shown in order to visualise the long-term picture of each instrument for the totality of the data available and not only the coincidences to GOME-2. Hence the stability of each instrument and algorithm behaviour may be examined. The comparative graphs are ordered from top to bottom in launch date from the one furthest back in time to the present. In order to create as homogeneous and hence comparable graphs possible, these contour representations were created with a spread of 0.2 of the year [i.e. one and a half months approximately] for the x-axis and 30 degrees in latitude for the y-axis. The original data were averaged with a one month spacing in time and 15 degrees in latitude. A common feature for all graphs which should be discussed here is the high negative values [more than -2.5%] around 15 degrees North which are due to the station of Bangkok, the sole station of the belt, which presents a near-constant ground-based over-estimation from year 2005 onwards. This feature may appear more pronounced in some figures than others depending on the averaging/binning performed as needed. The station is not excluded from any comparisons.

In the upper left of Fig. 1, the near 15 years of GOME total ozone monitoring is presented with the large gaps in the southern hemisphere after year 2003 due to the ERS-2 tape recorder failure. The gaps at the high latitudes, also noticeable for the other instruments are due to the lack of ground-based stations, and not a satellite effect. A definite seasonal effect persists through the years with lows [underestimation] during the summer months for the Northern Hemisphere. The general picture appears to be that the GOME measurements oscillate between over- and under-estimating the ground based estimates between -0.5% and 1% depending on the latitude belt and the season. This seasonal dependency northwards and southwards of 40° has also been reported in [*Balis et al.,* 2007a] with an amplitude that does not exceed 1%−1.5% for the Dobson comparisons. In the upper right, a similar structure can be observed for the SCIAMACHY comparisons which start at the end of year 2002 with some instrumental issues still lingering appearing as the

328 strong overestimations in all latitude bands for those months. From mid-2003 onwards
329 the northern middle latitudes demonstrate a seasonally affected underestimation of
330 around -1.5% whose amplitude also shows interannual variability whereas the
331 southern middle and high latitudes over-estimate by around 1%. These findings agree
332 very well with the validation analysis presented in *Lerot et al.*, 2009 even though the
333 set of ground-based stations used there is not entirely the same as the one used in this
334 study. In the middle left panel, the OMI_TOMS comparisons display the most
335 homogeneous character of all instruments, with values that revolve around the zero
336 difference [light green colours denote ± 0.5%], no spikes at the high latitudes and a
337 persistent slight understimation above 30° - 60° N. A different picture in the middle
338 right panel for the OMI_DOAS comparisons presenting the largest overestimates by
339 2-4% compared to the ground truth for the high latitudes of both Hemispheres for the
340 summer months, underestimates for the winter months and in general shows a
341 variable structure with problems for high SZA cases as well. There appears also to be
342 a general change in the comparative behaviour between ground and OMI_DOAS
343 from year 2009 which shown more prominently in the time series plots presented
344 below, a feature also observed for the Brewer comparisons [not shown here.] These
345 findings agree well with *Balis et al., 2007b*, who found the OMI-TOMS data product
346 of high overall quality with no significant dependence on solar zenith angle or
347 latitude. They showed as well that the OMI-DOAS data product systematically
348 overestimated the total ozone values in the high latitudes of the Southern Hemisphere
349 as well as a significant dependence on solar zenith angle. Finally, in the lower panel,
350 GOME-2 exhibits a similar behavior as GOME and SCIAMACHY with the seasonal
351 alteration between over- and under-estimating in the mid- to high latitudes. As shown
352 also in *Loyola et al., 2011*, the GOME-2 total ozone data obtained with GDP 4.4
353 slightly underestimates ground-based ozone by about 0.5% to 1% over the middle
354 latitudes of the Northern Hemisphere and slightly overestimates by around 0.5% over
355 the middle latitudes in the Southern Hemisphere.

356

357 3.1.2 **Long term stability**

358

359 Focusing on the time series of the differences as a mean over the NH stations, in
360 Figure 2 the time evolution of the behaviour of each instrument is shown, alongside

the standard deviation of the daily points which are included in the monthly mean value. In the same order as before, the GOME differences is shown on the upper left with the obvious seasonality with peak-to-peak that revolves around the zero line. SCIAMACHY in the upper right, shows exactly the same patterns as GOME whereas the OMI_TOMS differences in the middle left show a more or less flat behaviour as the years progress revolving around a mean of -1% and no pronounced seasonal effects. OMI_DOAS follows the GOME and SCIAMACHY seasonality peaks until mid-2009 where the differences show a noticeable change from revolving around the zero line, to an over-estimation of between 1 and 2%. The GOME-2 picture is very similar to that of the rest of the total ozone retrievals using the DOAS algorithm apart from the fact that the seasonal peak-to-peak differences go from -2% to 0%. The seasonality effect apparent in all DOAS algorithms [i.e. in all datasets shown apart from OMI_TOMS] can, for most part, be attributed to the fact that the satellite algorithms account for differences in effective temperature whereas the ground-based instruments use a steady temperature for the ozone cross-sections. A secondary effect arises from the fact that the DOAS algorithms cannot fit well the observed features at high SZAs, which appears to be both a seasonal and geometrical issue. Hence, the common features seen in Figure 2 between all algorithms apart from the OMI_TOMS one.

3.1.3 Seasonal variability

Another way to discern possible issues is to investigate the contour representation of the differences on a seasonal basis, as presented in Figure 3. The layout of this Figure is as per the previous two figures. For the visualization needs of this Figure, a 1/12 per annum radius in time was used as well as a 10 degrees radius in latitude. In the upper left, the sixteen years of GOME create a smooth and clear image which shows that for the Northern middle and high latitudes the satellite overestimates by around 1% for the winter and autumn months and underestimates by the same amount for the summer months. The Southern tropical belt around 20-30° appears a zone of underestimation of 1% whereas for the higher Southern latitudes the situation again reverses with a progressive increase in over-estimation as the Antarctic

394   stations are encountered which reaches the levels of 3 to 4%. This GOME

395   overestimation in polar latitudes during winter can probably be reduced by applying

396   GDP 4.4 (no addition of ghost column for snow/ice conditions). In the upper right, for

397   SCIAMACHY, a similar picture is detected for the Northern Hemisphere albeit with

398   more pronounced features: in the northern spring and summer-time mid-latitudes the

399   underestimation reaches -2% whereas the winter months also show a higher over-

400   estimations. For the Southern Hemisphere the pattern changes somewhat with the

401   tropical zone overshooting by around 1% for all seasons and the middle and high

402   latitudes overestimating up to 2-3% for the summer months and underestimating by

403   1% for the winter ones. In the middle left, the OMI_TOMS shows no seasonal or SZA

404   issues with a constant underestimation of -0.5% for all months and latitudes.

405   Conversely, in the middle right, OMI_DOAS shows a similar over- to under-

406   estimating pattern as SCIAMACHY with different amplitudes with, interestingly,

407   quite high values reaching 3-4% for the spring Antarctic region. Finally, in the lower

408   left, GOME-2 shows a strong, around -2%, underestimation for the tropical belt

409   around ±30° for all seasons which persists for higher Southern latitudes for the winter

410   months. The Equatorial belt missing from this plot is due to the fact that the stations

411   that belong to that belt i.e. Natal/Brazil, and Nairobi/ Kenya, provide data only up to

412   2004 and 2000 respectively.

413

414

415   **3.2   Joint analysis and intercomparison**

416   In the following section the comparison between GOME-2 and the other four

417   satellite datasets is demonstrated through a composite Figure with eight panels which

418   follow the same colour-coding format. Common days of data between the GOME

419   record and each of the other instruments are used. In the first row of Figure 4 the

420   percentage differences between satellite and co-located ground-based measurements

421   have been grouped in 10° bins in latitude. In the second row, the differences have

422   been grouped in 5° bins in solar zenith angle. In the third row, the cloud top pressure,

423   *CTP*, dependency for each of the satellites is examined for bins of 50 mbars and in the

424   fourth and final row, the cloud fraction in bins of 5%. These plots will be hereafter

425   referred to as *Latitudinal variability, SZA variability, CTP variability* and *cloud*

426   *fraction variability* respectively.

427 For the case of the *Latitudinal variability* and the Dobson comparisons [Fig. 4 top

428 left]: a very close agreement for the NH and the tropics is observed in the behaviour

429 of all five algorithms up to 50°N. From then and northwards OMI_DOAS presents a

430 steady 1-2% over-estimation and GOME deviates at the Arctic stations with an over-

431 estimation of more than 2%. The other three algorithms present a very similar picture.

432 In the SH the comparisons are more diverse: GOME is under-estimating near -0.5%

433 around the Equator and tropics and reaching -2% in the Antarctic. A very similar

434 behaviour is observed by SCIAMACHY and OMI_TOMS. OMI_DOAS is constantly

435 over-estimating by between 1 and 3% whereas GOME-2 shows a more constant

436 behaviour around the zero line with the exception of the Antarctic where the

437 differences reach 3%. For the Brewer comparisons [Fig. 4 top right], the situation is

438 more homogeneous with no latitudinal dependency seen in any of the algorithms and

439 a mean of -2% for GOME-2 and OMI_TOMS, a mean around -1% for GOME and

440 SCIAMACHY and a mean of around zero for OMI_DOAS. This can be attributed to

441 the fact that most Brewer stations fall around the middle latitude regions were the

442 observational geometries and TOC ranges are far more favourable for constant, un-

443 biased ground-based time series.

444 For the case of the *SZA variability* and the Dobson comparisons [second row left]: all

445 algorithms show a similar picture with under-estimation for the low SZAs, over-

446 estimation for the high SZAs and an obvious SZA dependency. What differentiates

447 one instrument from the other is the magnitude of the dependency; GOME-2 and

448 OMI_TOMS show the least amount of dependency with values ranging between -

449 0.5% for the low and 0.5% for the high SZAs. OMI_DOAS seems to show the worse

450 behaviour with a dependency that starts around 0% in difference and rises to 3% for

451 SZAs higher than 80°. GOME and OMI_DOAS demonstrate a dependency in

452 between these two extremes. For the Brewer comparisons [second row right], all

453 algorithms show the same mild positive dependency in SZA with differences that start

454 around -2% for the low SZA and rise to 0-2% for the high SZA apart from

455 OMI_TOMS which is showing a more stable albeit negative dependency between -

456 0.5% and -2% for all SZAs.

457 For the case of the *CTP variability* and the Dobson comparisons [third row left]:

458 GOME-2 and OMI_TOMS show no dependency whatsoever and average values

459 around 0%. SCIAMACHY shows a mild negative dependency, moving from a 2%

460 over-estimation for low CTP to a -1% under-estimation for high CTP. GOME and

461   OMI_DOAS show the strongest dependencies with averages ranging between 4% and

462   -2%. For the Brewer comparisons [third row right] a near-exact situation can be seen.

463   A point to consider when examining the very low [< 200mbars] and very high [>

464   800mbars] CTP cases is the amount of data points that have been used in these graphs

465   where for example for the case of the GOME measurements only 25 points make up

466   the 200mbar bin, 60 the 300 mbar bin whereas there exist around 600 points for the

467   800 mbars bin.

468   For the case of the *cloud fraction variability* and the Dobson comparisons [bottom

469   left]: no dependency and near-zero comparative values for all satellites apart from

470   OMI_DOAS which shows a constant 1% positive offset for all cloud fractions. Near-

471   similar picture for the Brewer comparisons with all algorithms around the -1%

472   negative offset.

473   The comparisons as function of *CTP variability* and *cloud fraction variability* agree

474   well with the results from *Antón and Loyola*. 2011.

475   In Tables 2 and 3, some statistics for the differences between satellite and ground-

476   based measurements are given for distinct cases of latitudinal and SZA belts. In

477   particular, three latitude bands are shown; the tropical zone, from 0° to 30° N, a

478   middle latitude one, from 30° to 60° N and a polar one, from 60° to 90° N, as well as

479   three SZA bands; low SZA, from 0° to 25°, middle SZA from 25° to 70° and high

480   SZA from 70° to 90°. Table 2 shows the statistics for the Brewers and Table 3 the

481   statistics for the Dobson instruments. The seemingly high standard deviation is due to

482   the fact that raw daily measurements were used for these statistics and not already

483   binned, and hence smoothed out, data.

484   Delving deeper into the comparative behaviour of the GOME-2 ozone record

485   compared to the other algorithms, the direct scatter plots of the common data points

486   between the satellites for the Dobson locations only are given in Figure 5. With

487   GOME-2 always on the y-axis, the scatter against GOME is shown in the upper left,

488   OMI_TOMS in the upper right, OMI_DOAS in the lower left and SCIAMACHY in

489   the lower right. The different colours denote the SZA values associated with the total

490   ozone columns. The first point to note is the excellent correlation level which in all

491   cases has an R^2 of 0.98 and the data points in all cases fall nicely in the y=x line. No

492   obvious dependency of the total ozone columns on the SZA can be seen. For the high

493   SZAs [orange colour] associated with the low Antarctic total ozone values the

494   GOME-2 data under-estimates the GOME and OMI_DOAS data, while agreeing well

495   with OMI_TOMS and SCIAMACHY. The least deviation from the y=x line can be
496   seen in the comparisons with GOME [upper left] and the highest with OMI_DOAS
497   [lower left.] In the OMI_DOAS comparisons numerous outlier points are observed
498   irrespective of the associated SZA which points to the fact that the reason behind the
499   disagreement is not due to the SZA treatment of the algorithms.
500
501   **4   Summary and Conclusions**
502
503   In the current paper we have assessed the stability and compatibility of five years of
504   Global Ozone Monitoring Experiment-2/Metop-A total ozone columns against that of
505   GOME/ERS, OMI/Aura and SCIAMACHY/Envisat through an extensive inter-
506   comparison and validation exercise using as reference Brewer and Dobson ground-
507   based measurements. Over the background truth of the ground-based measurements,
508   the total ozone columns are inter-evaluated using a suite of established validation
509   techniques and the main findings follow;
510
511   i.   On average, GOME-2 data underestimate GOME data by about 0.80%, and
512   underestimate SCIAMACHY data by 0.40%. There is no seasonal dependence of
513   the differences between GOME-2, GOME and SCIAMACHY. The latter is
514   expected since the three data sets are based on similar algorithms (GDP 4.x). This
515   underestimation of GOME-2 is within the uncertainty of reference ground-based
516   data used in the comparisons.

517   ii.   On average, GOME-2 data show no dependency with respect to the cloud top
518   pressure and the cloud fraction, with discrepancies between the -1% and zero
519   levels. The same picture is observed for the OMI_TOMS data. The rest of the
520   algorithms show varying levels of dependency, especially for high clouds, bearing
521   in mind the sparcity of data at the low cloud top pressure values.

522   iii. On average, GOME-2 data show very little SZA dependency and only for angles
523   larger than 75°, maintaining a constant bias compared to the ground-based data.
524   Marked is the improvement over the GOME dataset.

525   iv.   On average, GOME-2 data underestimate OMI_DOAS (collection 3) data by
526   1.28%, without any significant seasonal dependence of the differences between
527   them. The lack of seasonality might be expected since both GDP 4.4 and

528   OMI_DOAS are DOAS-type algorithms and both consider the variability of the
529   stratospheric temperatures in their retrievals.

530 v.   On average, GOME-2 data and OMI_TOMS (collection 3) data have almost no
531   bias (GOME-2 underestimates by 0.10%).

532 vi. Overall, GOME-2 total ozone data agree at the ±1% level with the standard
533   ground-based measurements as well as other satellite instrument datasets and
534   therefore are well suited to be incorporated and hence continue the satellite long-
535   term global total ozone record needed among others for climate monitoring
536   studies.

537

Acknowledgments

539

547

References

549

550   Antón, M., M. E. Koukouli, M. Kroon, R. D. McPeters, G. J. Labow, D. Balis, and A.
551   Serrano, Global validation of empirically corrected EP-Total Ozone Mapping
552   Spectrometer (TOMS) total ozone columns using Brewer and Dobson ground-
553   based   measurements,   *J.   Geophys.   Res.*,   115,   D19305,
554   doi:10.1029/2010JD014178, 2010.

555   Antón, M., and D. Loyola, Influence of cloud properties on satellite total ozone
556   observations, *J. Geophys. Res.*, 116, D03208, doi:10.1029/2010JD014780,
557   2011.

558   Balis, D., M. Kroon, M. E. Koukouli, E. J. Brinksma, G. Labow, J. P. Veefkind, and
559   R. D. McPeters, Validation of Ozone Monitoring Instrument total ozone column
560   measurements using Brewer and Dobson spectrophotometer ground-based
561   observations, *J. Geophys. Res.*, 112, D24S46, doi:10.1029/2007JD008796,
562   2007a.

563   Balis, D., J-C. Lambert , Van Roozendael M., D. Loyola, R. Spurr, Y. Livschitz, P.
564   Valks, T. Ruppert, P. Gerard, J Granville and V. Amiridis, Ten years of
565   GOME/ERS2 total ozone data—The new GOME data processor (GDP) version
566   4: 2. Ground-based validation and comparisons with TOMS V7/V8, *J. Geophys.*
567   *Res.*, 112, D07307, doi:10.1029/2005JD006376, 2007b.

568   Bass A.M., and R.J. Paur, The ultraviolet cross-sections of ozone: I. The
569   measurements in Atmospheric ozone (Ed. C.S. Zerefos and A. Ghazi), Reidel,
570   Dordrecht, Boston, Lancaster, pp. 606-610, 1985.

571   Bhartia, P.K., C.G. Wellemeyer, S.L. Taylor, N. Nath, and A. Gopolan, Solar
572   backscatter ultraviolet (SBUV) version 8 profile algorithm, in Proceedings of
573   the Quadrennial Ozone Symposium, Kos, Greece, 1-8 June 2004, 295-296,
574   2004.

575   Bogumil, K., Orphal, J., Homann, T., Voigt, S., Spietz, P., Fleischmann, O. C., Vogel,
576   A., Hartmann, M., Bovensmann, H., Frerick, J., and Burrows, J. P.:
577   Measurements of molecular absorption spectra with the SCIAMACHY pre-
578   flight model: instrument characterization and reference data for atmospheric
579   remote sensing in the 230–2380 nm region, *J. Photochem. Photobiol. A.,* 157,
580   167–184, 2003.

581   Bovensmann, H., Burrows, J., Buchwitz, M., J. Frerick, S. Noël, V. V. Rozanov, K.
582   V. Chance, A. P. H. Goede, SCIAMACHY: Mission objectives and
583   measurement modes, *J. Atmos. Sci.*, 56, 2, 127–150, 1999.

584   Burrows, J., M. Weber, M. Buchwitz, V. Rozanov, A. Ladstätter-Weißenmayer, A.
585   Richter, R. DeBeek, R. Hoogen, K. Bramstedt, K.-U. Eichmann, M. Eisinger
586   and D. Perner: The Global Ozone Monitoring Experiment (GOME): Mission
587   concept and first scientific results, *J. Atmos. Sci.*, 56, 151–175, 1999.

588   Burrows, J., A. Richter, A. Dehn, B. Deters, S. Himmelmann, S. Voigt, and J. Orphal,

589   Atmospheric remote sensing reference data from GOME: Part 2. Temperature-

590   dependent absorption cross-sections of O3 in the 231 – 794 nm range, *J. Quant.*

591   *Spectrosc. Radiat. Transfer*, 61, 509– 517, 1999b

592   Lerot C, Van Roozendael, M., van Geffen, J., et al., Six years of total ozone column

593   measurements from SCIAMACHY nadir observations, Atmos. Meas. Tech., 2,

594   87-98, 2009.

595   Levelt P.F., G.H.J. van den Oord, M.R. Dobber, A. Malkki, H. Visser, J. de Vries, P.

596   Stammes, J.O.V. Lundell and H. Saari, "The Ozone Monitoring Instrument",

597   IEEE Trans. Geosc. Rem. Sens., 44 (5), 1093-1101, 2006.

598   Loyola, D. G., M. E. Koukouli, P. Valks, D. S. Balis, N. Hao, M. Van Roozendael, R.

599   J. D. Spurr, W. Zimmer, S. Kiemle, C. Lerot and J-C. Lambert, The GOME-2

600   total column ozone product: Retrieval algorithm and ground-based validation, *J.*

601   *Geophys. Res.*, 116, D07302, doi:10.1029/2010JD014675, 2011

602   Munro, R., M. Eisinger, C. Anderson, J. Callies, E. Corpaccioli, R. Lang, A.

603   Lefebvre, Y. Livschitz, and A. Perez Albinana: GOME-2 on METOP: From in-

604   orbit verification to routine operations, paper presented at EUMETSAT

605   Meteorological Satellite Conference, Helsinki, Finland, 12–16 June 2006.

606   Schoeberl M., A. Douglass, E. Hilsenrath, P.K. Bhartia, R. Beer, J. W. Waters, M.

607   Gunson, L. Froidevaux, J. Gille, J. Barnett, P. Levelt, and P. DeCola, Overview

608   of the EOS Aura Mission, IEEE Trans. Geo. Rem. Sens., 44, 1066–1074,

609   doi:10.1109/TGRS.2005.861950, 2006.

610   Valks P., D. Loyola, N. Hao, M.Rix and S. Slijkhuis, Algorithm Theoretical Basis

611   Document for GOME-2 Total Column Products of Ozone, NO_2, tropospheric

612   NO_2, BrO, SO_2, H_2O, HCHO, OClO and Cloud Properties, DLR/GOME-

613   2/ATBD/01, Iss/Rev: 2/E, http://atmos.caf.dlr.de/gome2/docs/DLR_GOME-

614   2_ATBD.pdf, accessed 15/12/2011, 2011

615   Van Roozendael, M., P.Peters, P.C.Simon, H.K.Roscoe, A.E.Jones, L.Bartlett,

616   G.Vaughan, F.Goutail, J-P.Pommereau, E.Kyro, C.Whalstrom, G.Braathen and

617   P.C.Simon, Validation of ground-based visible measurements of total ozone by

618   comparison with Dobson and Brewer spectrophotometers, *J. Atmos. Chem.,* 29,

619   55-83, 1998.

620 Van Roozendael M., D. Loyola, R. Spurr, D. Balis, J-C. Lambert, Y. Livschitz, P.

621   Valks, T. Ruppert, P. Kenter, C. Fayt and C. Zehner (2006), Ten years of

622   GOME/ERS-2 total ozone data—The new GOME data processor (GDP) version

623   4: 1. Algorithm description, *J. Geophys. Res.*, 111, D14311,

624   doi:10.1029/2005JD006375

625 Veefkind, J.P., J.F. de Haan, E.J. Brinksma, M. Kroon and P.F. Levelt, Total Ozone

626   from the Ozone Monitoring Instrument (OMI) Using the DOAS technique,

627   IEEE   Trans.   Geo.   Rem.   Sens.,   44,   5,   1239-1244,

628   doi:10.1109/TGRS.2006.871204, 2006.

629

630   **TABLES**

631

632   **Table 1.** Main characteristics of the GOME-2/MetOp GOME/ERS-2, SCIAMACHY

633   and OMI instruments relevant to the total ozone column products.

634

	GOME/ERS-2	SCIAMACHY	OMI	GOME-2/MetOp
Principle	**UV/VIS grating spectrometer**	**UV/VIS/NIR grating spectrometer**	**UV/VIS grating spectrometer**	**UV/VIS grating spectrometer**
Detectors	**Reticon linear diode array**	**Reticon linear diode array**	**2-dimensional CCD**	**Reticon linear diode array**
Spectral resolution	**0.20 nm**	**0.26 nm**	**0.45 nm**	**0.26 nm**
Spatial resolution (default)	**320 x 40 km^2**	**60 x 30 km^2**	**Up to 13 x 24 km^2**	**80 x 40 km^2**
Swath width	**960 km**	**960 km**	**2600 km**	**1920 km**
Dataset span	**1995-2011**	**2002-2011**	**2004-2011**	**2007-2011**
Eq. crossing time	**10:30 LT**	**10:00 LT**	**13:30 LT**	**09:30 LT**
Level-0-to-1b alg.	**GDP L01 4.0**	**IPF 6.03**	**OML1BRUG (v003)**	**GOME-2 PPF 4.x**
Level-1-to-2 alg.	**GDP 4.1**	**SDOAS (SGP 5.0)**	**OMDOAO3 v1.0.5 & OMTO3 v1.1.0**	**GDP 4.4**

635   * In addition to the parameters listed here, the differential signal-to-noise

636   characteristics of the instruments can have an impact on the total ozone column

637   retrieval as well.

638

639

640   **Table 2.** The average differences between satellite and ground-based instrument for

641   the five datasets shown in this paper. The mean and standard deviation for the

642   latitudinal and the SZA variability are given for the Brewer instruments for low,

643   middle and high latitudes and angles respectively.

	BREWER	
	LATITUDINAL VARIABILITY	SZA VARIABILITY

	Tropical [0-30°N]	Mid-Latitudes [30-60°N]	Polar [60-90°N]	Low [0-25°]	Middle [25-70°]	High [70-90°]
GOME-2	-2.0±2.4%	-1.9±2.4%	-1.5±3.0%	-2.1±2.4%	-1.8±2.4%	-0.4±3.2%
GOME	-1.7±2.6%	-1.0±2.8%	-0.02±3.4%	-1.8±2.7%	-0.6±2.8%	1.1±3.5%
OMI_TOMS	-0.8±2.2%	-1.0±2.1%	-1.5±2.4%	-0.8±2.1%	-1.0±2.4%	-1.1±4.3%
OMI_DOAS	-0.2±3.2%	-0.02±2.9%	-0.5±10.8%	0.03±3.3%	0.3±3.0%	1.1±9.7%
SCIAMACHY	-1.3±2.8%	-1.0±2.6%	-0.6±3.0%	-1.6±2.7%	-0.8±2.6%	0.3±3.5%

Table 3. The average differences between satellite and ground-based instrument for the five datasets shown in this paper. The mean and standard deviation for the latitudinal and the SZA variability are given for the Dobson instruments for low, middle and high latitudes and angles respectively.

	DOBSON					
	LATITUDINAL VARIABILITY			SZA VARIABILITY		
	Tropical [0-30°N]	Mid-Latitudes [30-60°N]	Polar [60-90°N]	Low [0-25°]	Middle [25-70°]	High [70-90°]
GOME-2	-1.3± 3.2%	-0.9±2.7%	-0.6±3.2%	-1.7±3.2%	-0.8±3.0%	0.7±5.8%
GOME	-1.3± 15.1%	-0.4±10.3%	0.6±4.0%	-1.4±2.2%	0.2±3.3%	2.0±6.3%
OMI_TOMS	-0.9±3.3%	-0.9±3.3%	-0.5±3.0%	-0.9±3.3%	-0.5±3.0%	0.06±3.8%
OMI_DOAS	-0.2± 4.0%	0.2±4.0%	1.3±4.7%	0.3±4.1%	0.9±3.9%	2.8±5.9%
SCIAMACHY	-1.1±3.6%	-0.5±3.1%	-0.4±3.8%	-1.0±3.6%	0.05±3.6%	1.0±5.8%

FIGURE CAPTIONS

Figure 1. Contour representation of the difference between satellite and Dobson ground-based measurements for the five datasets discussed in this paper as a function of latitude and time. **Top left:** GOME. **Top right:** SCIAMACHY. **Middle left:** OMI_TOMS. **Middle right**: OMI_DOAS. **Bottom:** GOME-2.

Figure 2. Time series of the differences between satellite and Dobson ground-based measurements for the five datasets for the Northern Hemisphere stations only. **Top left:** GOME. **Top right:** SCIAMACHY. **Middle left:** OMI_TOMS. **Middle right**: OMI_DOAS. **Bottom:** GOME-2.

Figure 3. Contour representation of the percentage differences between satellite and Dobson ground-based total ozone measurements depicted as a function of solar zenith angle and season. **Top left:** GOME. **Top right:** SCIAMACHY. **Middle left:** OMI_TOMS. **Middle right**: OMI_DOAS. **Bottom:** GOME-2.

Figure 4. Comparisons of GOME-2 [purple], GOME [dark blue], OMI-TOMS [light blue], OMI-DOAS [light green] and SCIAMACHY [red] total ozone against the same ground-based measurements. Left column are the Brewer comparisons and the right column the Dobson comparisons. From top to bottom the dependence of the percentage differences as function of latitude, solar zenith angle, cloud top pressure and cloud fraction.

Figure 5. Direct scatter plot comparisons of the satellite total column at the overpass sites for the Dobson ground-based stations. Top row: GOME-2 [on the y-axis] to GOME [left plot] and OMI_TOMS [right plot.] Bottom row: GOME-2 [on the y-axis] to OMI_DOAS [left plot] and SCIAMACHY [right plot.] The points are colour-coded according to the SZA related to that measurement. The r-squared and y-intercept of the scatter line [red] are also given.

FIGURES
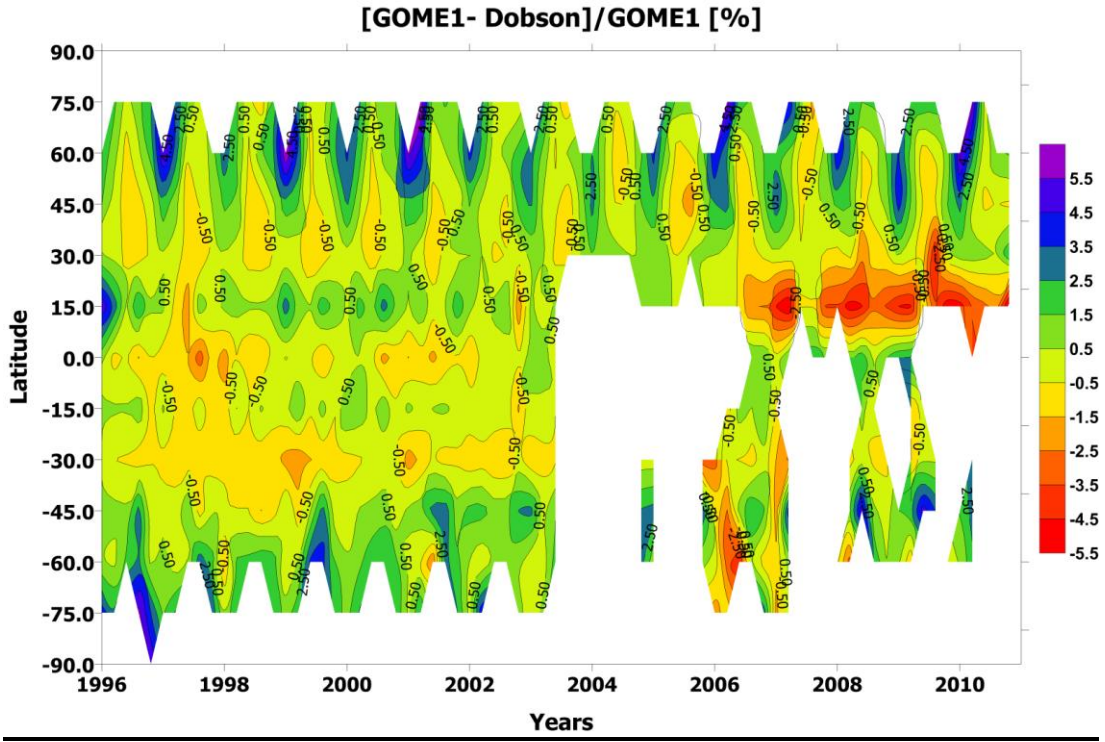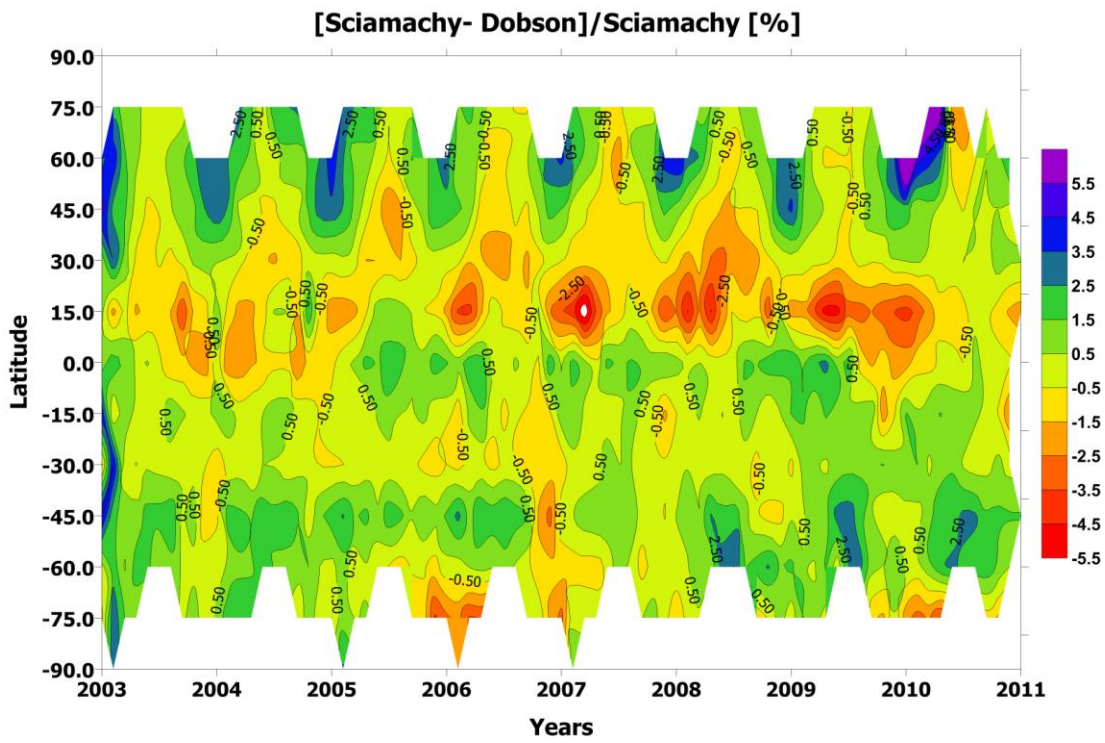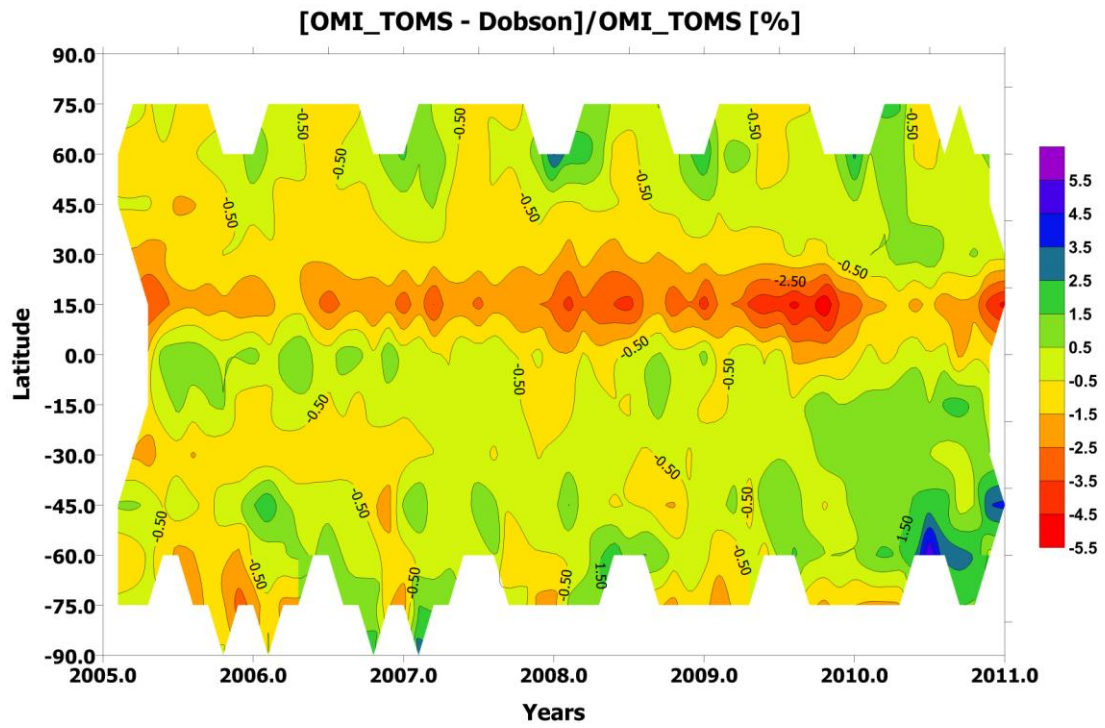
677

678

679   Figure 1 Top Left

680
681   Figure 1 Top Right

[OMI_TOMS - Dobson]/OMI_TOMS [%]

682
683   Figure 1 Middle Left

[OMI_DOAS - Dobson]/OMI_DOAS [%]

684
685   Figure 1 Middle Right

[GOME2- Dobson]/GOME2 [%]

686
687   **Figure 1 Bottom.**

NORTHERN HEMISPHERE

GOME1 GDP4.x

Trend per annum=   −0.0001+/−   0.0175

dobson

Created on Fri Jun 08 09:40:57 2012   Aristotle University of Thessaloniki

688
689   **Figure 2 Upper Left**

NORTHERN HEMISPHERE

SCIAMACHY

Trend per annum=   −0.0466+/−   0.0471

[SCIAMACHY−GROUND] / SCIAMACHY [%]

dobson
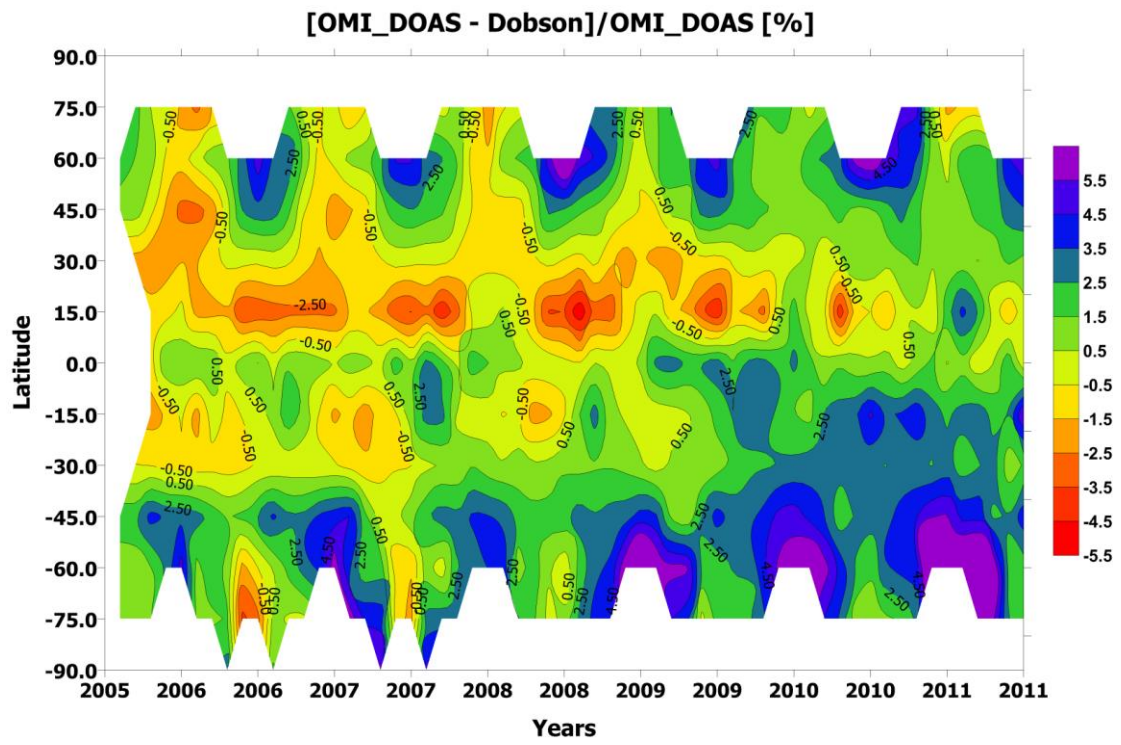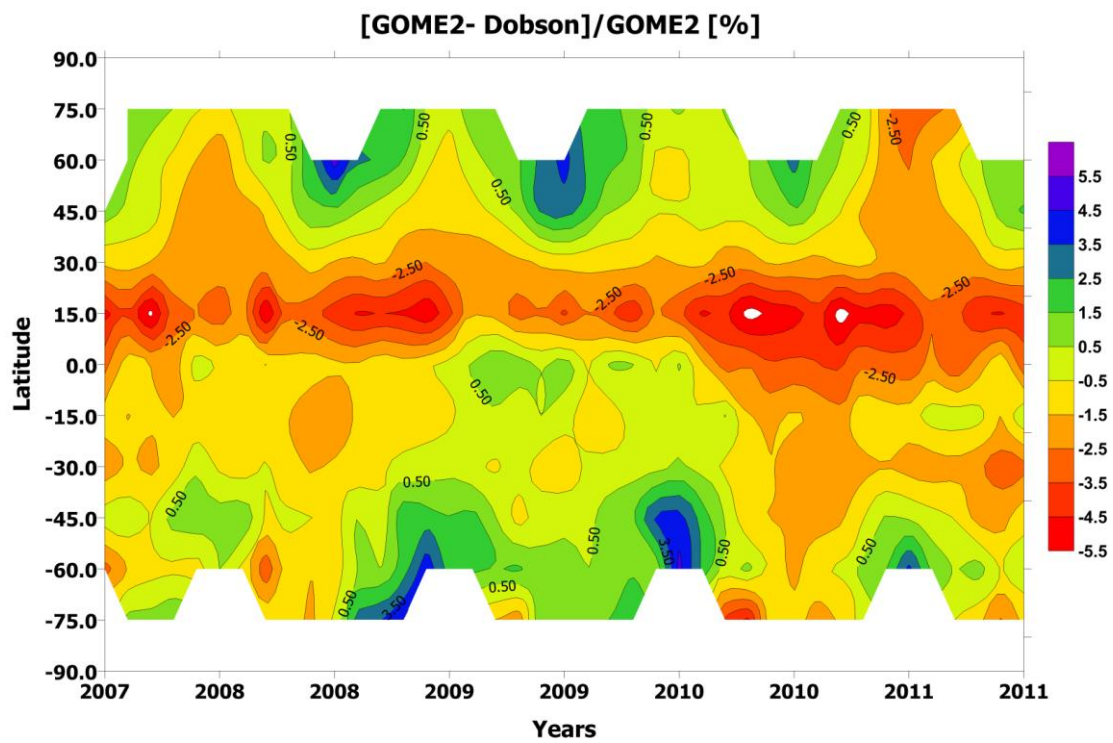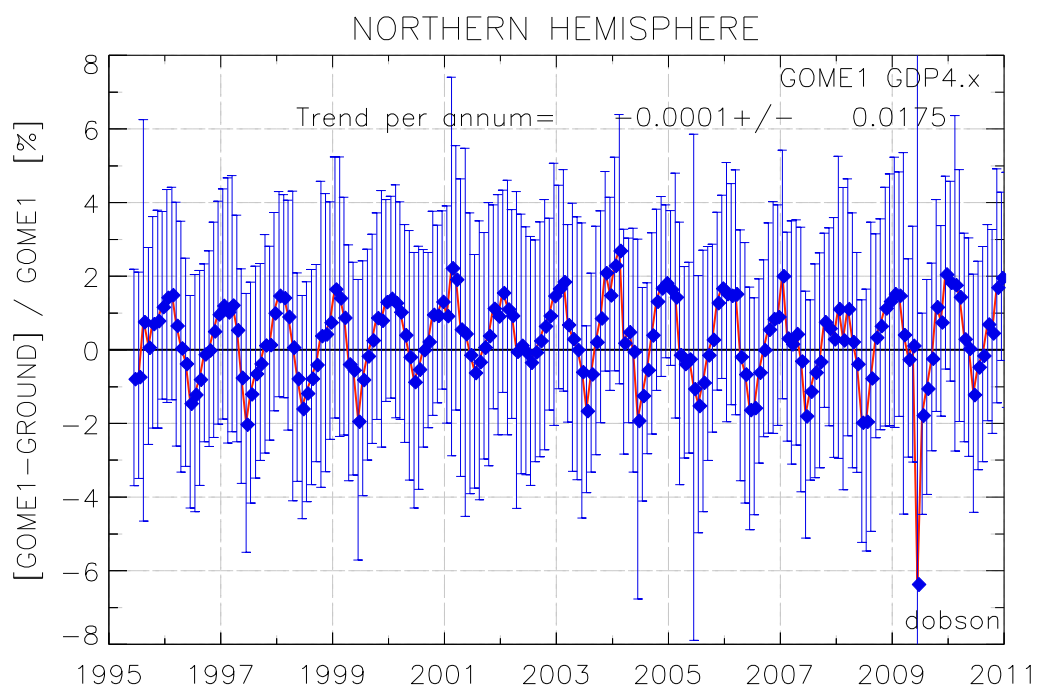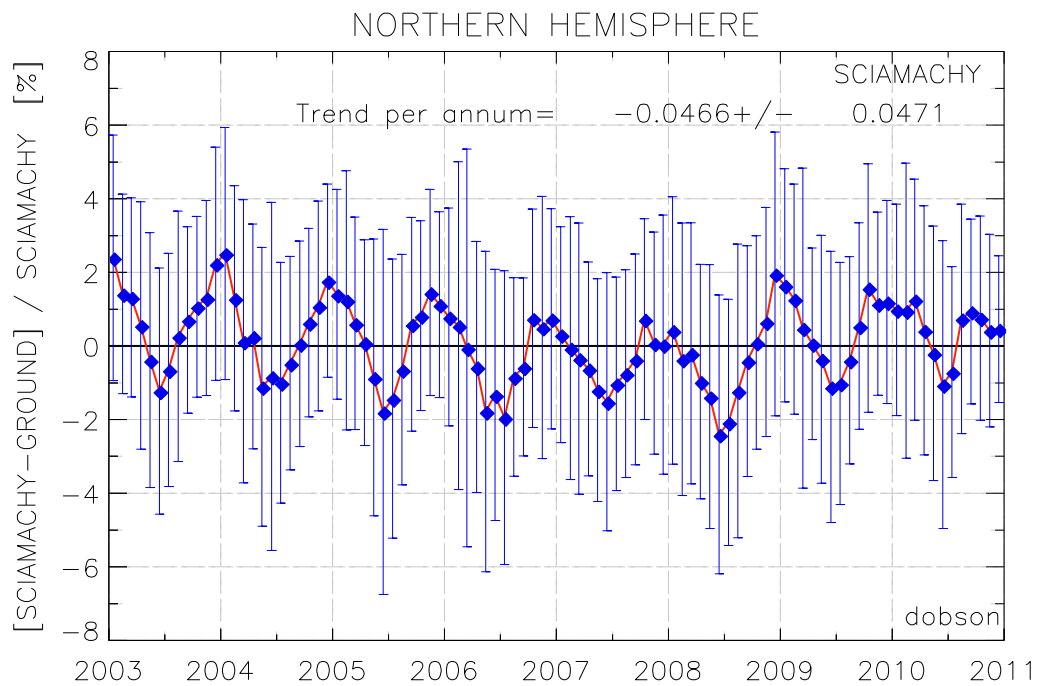
Created on Fri Jun 08 09:34:43 2012   Aristotle University of Thessaloniki
Figure 2 Upper Right

NORTHERN HEMISPHERE

OMI TOMS

Trend per annum=   0.0856+/−   0.0275

[OMI−GROUND] / OMI [%]

dobson
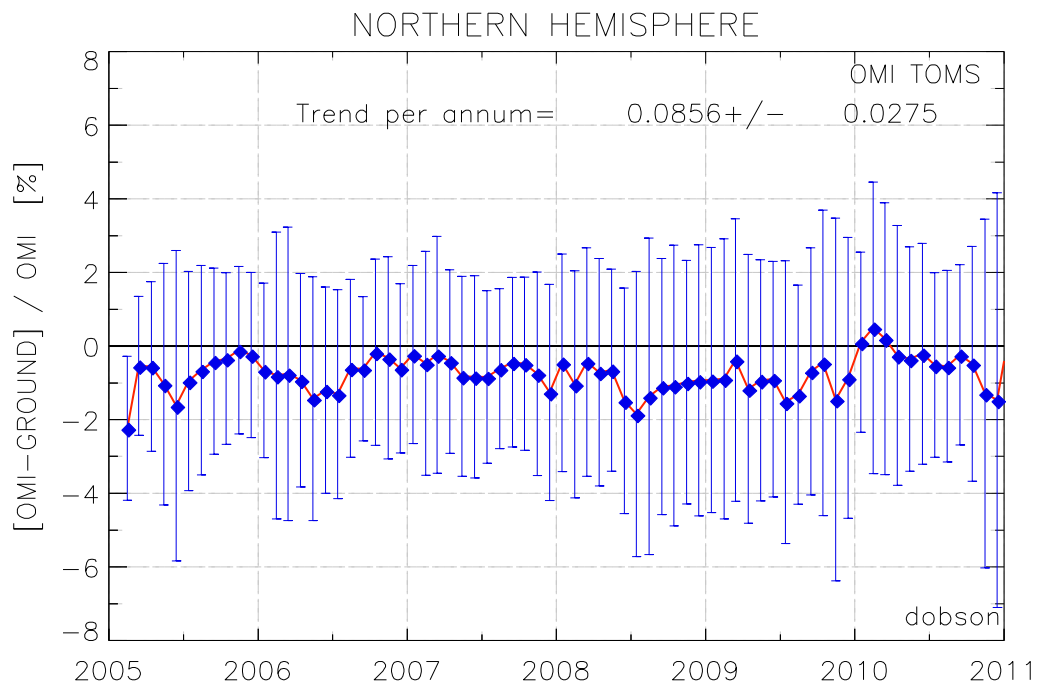
Created on Fri Jun 08 09:35:45 2012   Aristotle University of Thessaloniki
Figure 2 Middle Left

NORTHERN HEMISPHERE

OMI DOAS

Trend per annum=   0.0352+/-   0.0436

dobson
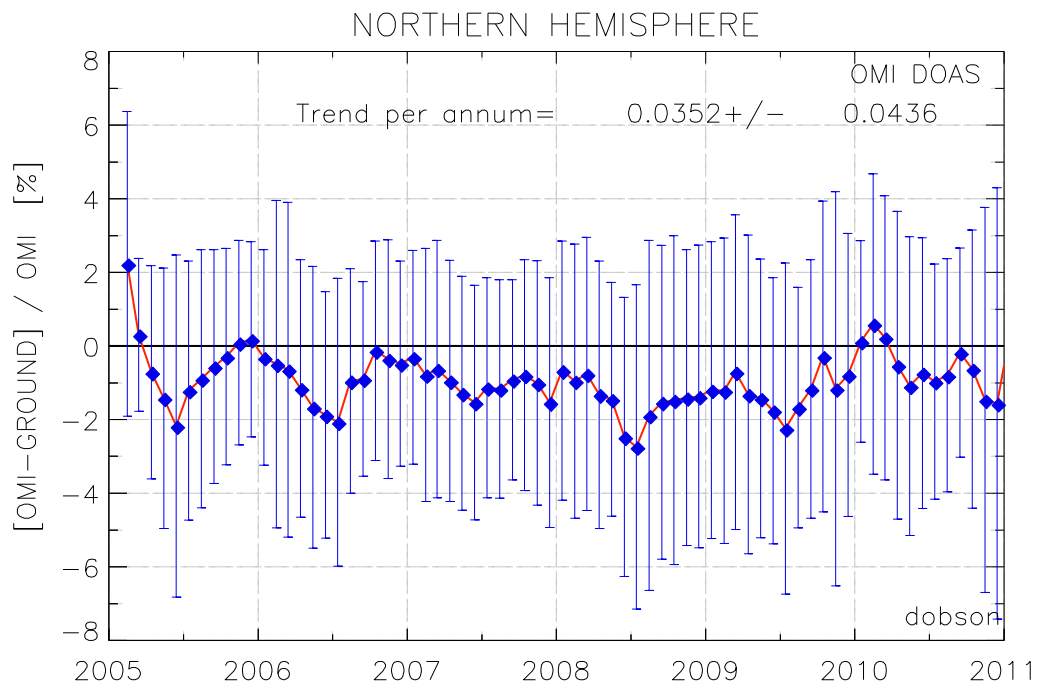
Created on Fri Jun 08 09:36:05 2012   Aristotle University of Thessaloniki

694
695 **Figure 2 Middle Right**

NORTHERN HEMISPHERE

GOME2 GDP4.4

Trend per annum=   0.0836+/-   0.0644

dobson
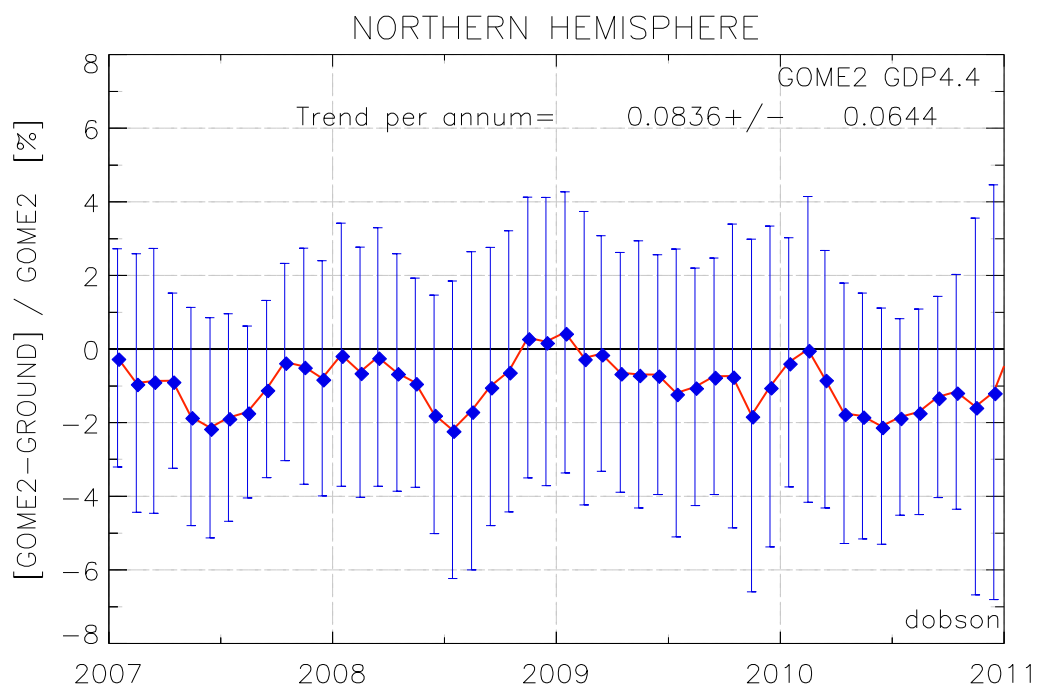
Created on Fri Jun 08 09:43:58 2012   Aristotle University of Thessaloniki

696
697 **Figure 2 Bottom**

[GOME1-GROUND] / GOME1 [%]
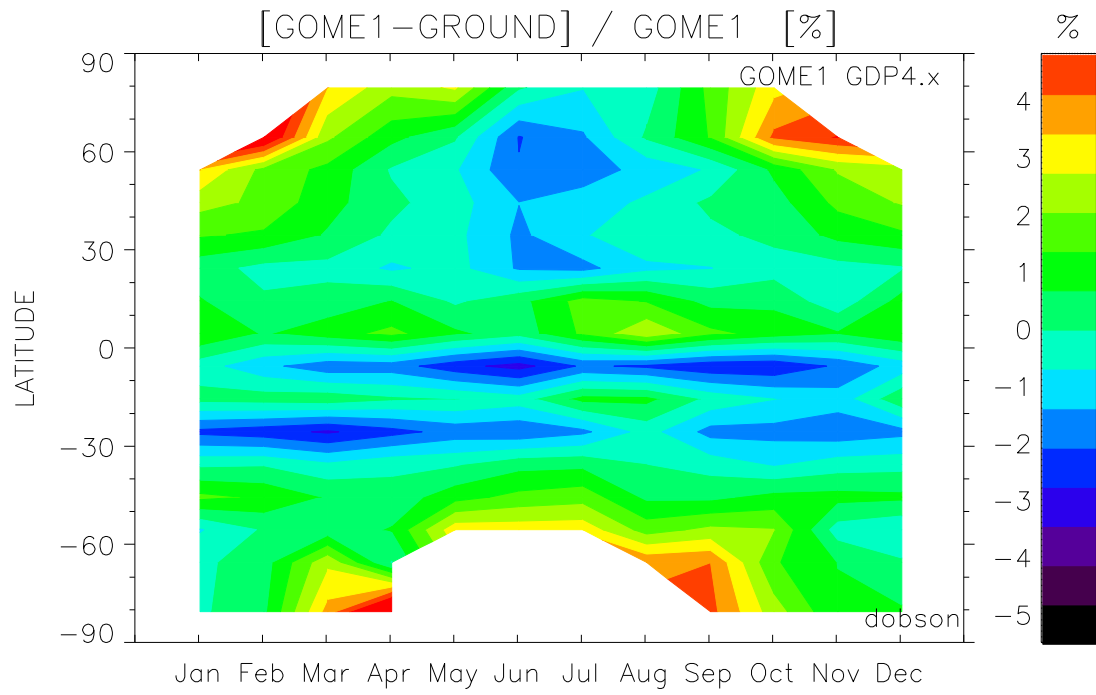
698
699 Figure 3 Upper Left

[SCIAMACHY-GROUND] / SCIAMACHY [%]
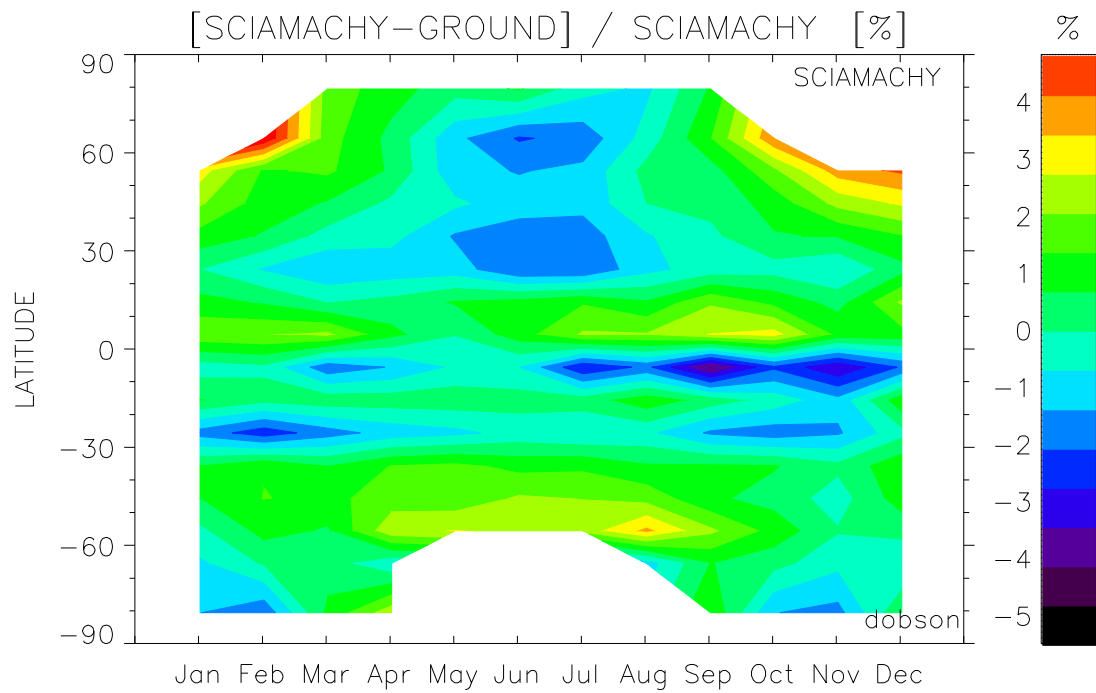
700
701 Figure 3 Upper Right

[OMI-GROUND] / OMI [%]

OMI TOMS

dobson
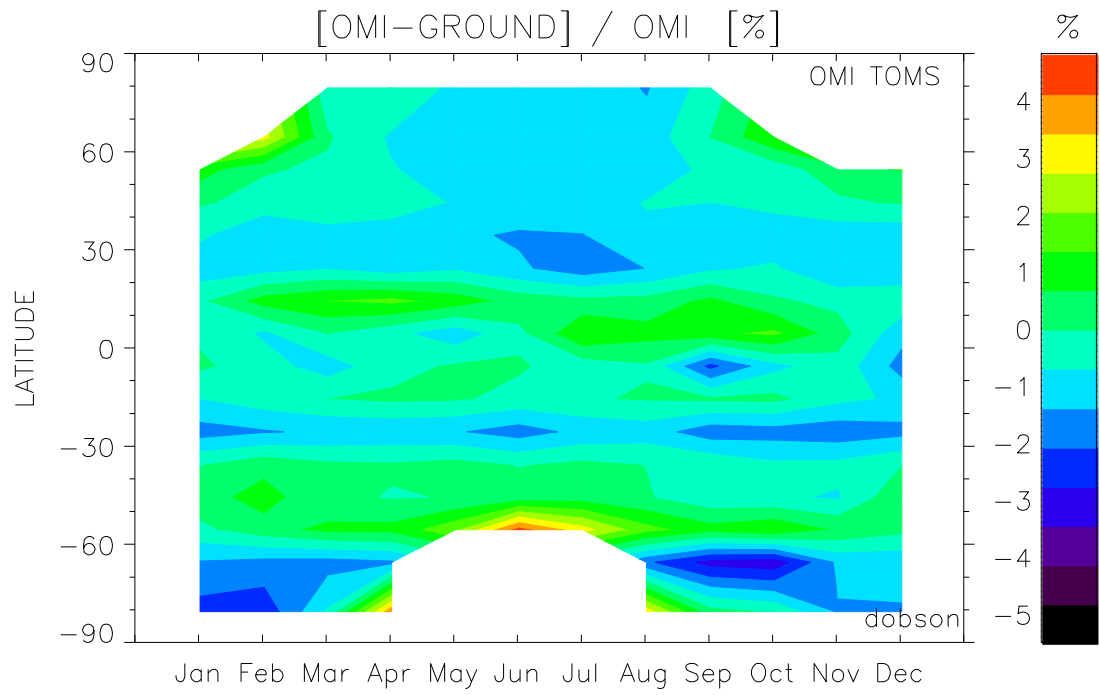
Created on Fri Jun 08 09:20:44 2012

702
703   **Figure 3 Middle Left.**

[OMI-GROUND] / OMI [%]

OMI DOAS

dobson
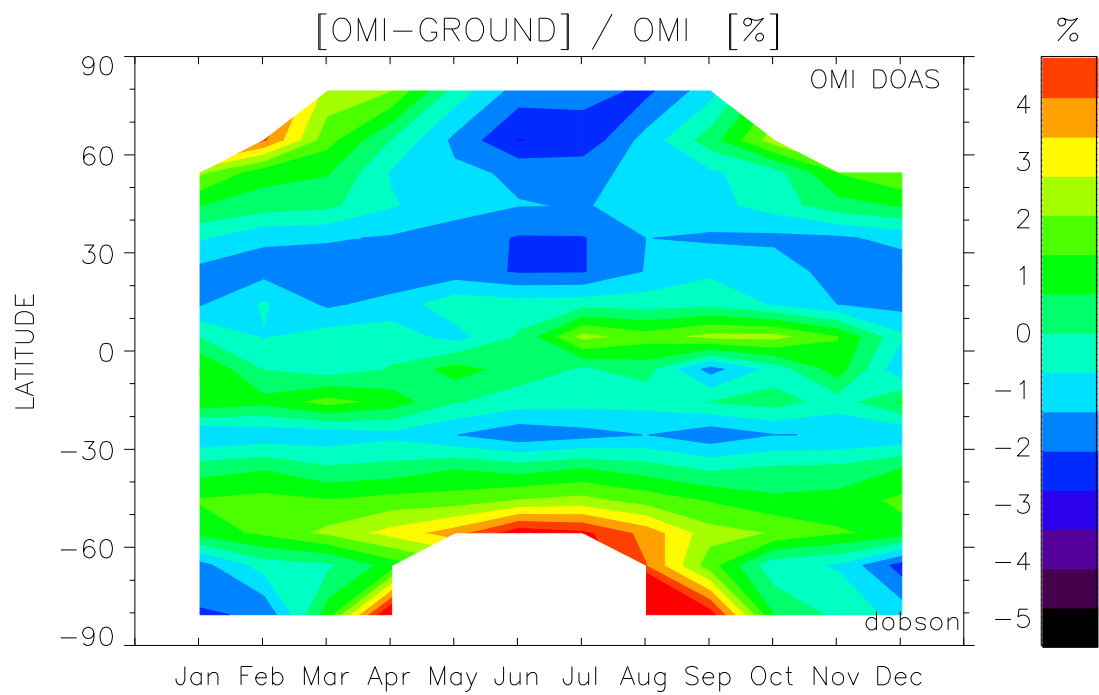
Created on Fri Jun 08 09:21:26 2012

704
705   **Figure 3 Middle Right**

[GOME2−GROUND] / GOME2 [%]

GOME2 GDP4.4

dobson
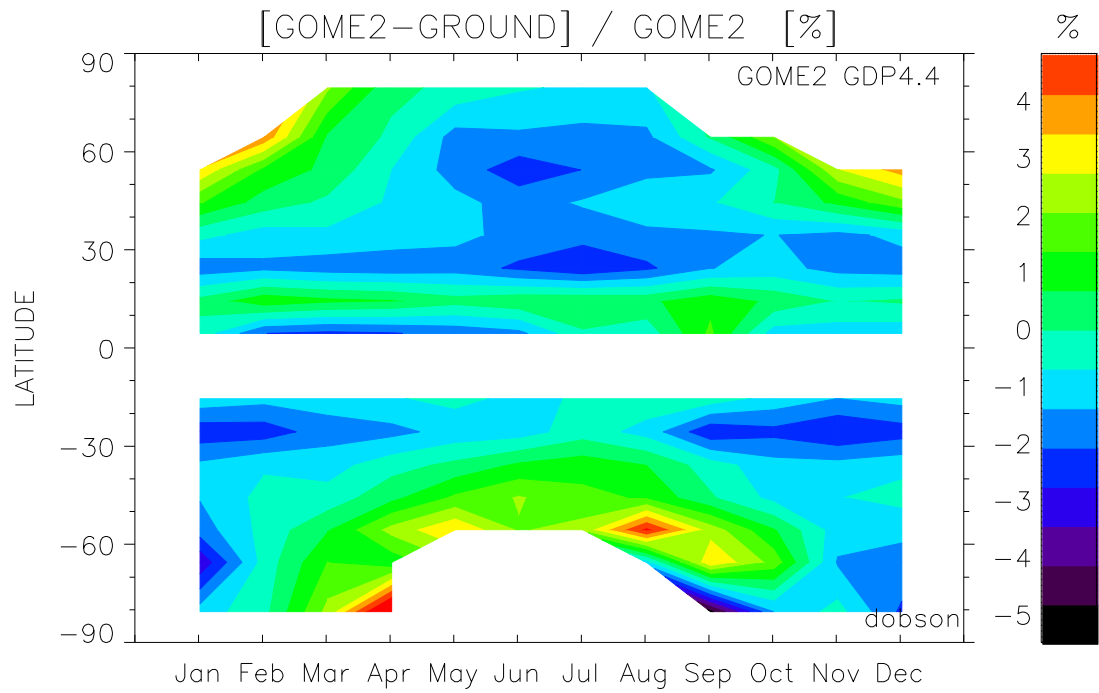
Created on Fri Jun 08 09:03:08 2012

706
707 **Figure 3 Bottom**

GOME2 GDP4.4
GOME1 GDP4.x
OMI_TOMS
OMI_DOAS
SCIAMACHY

brewer
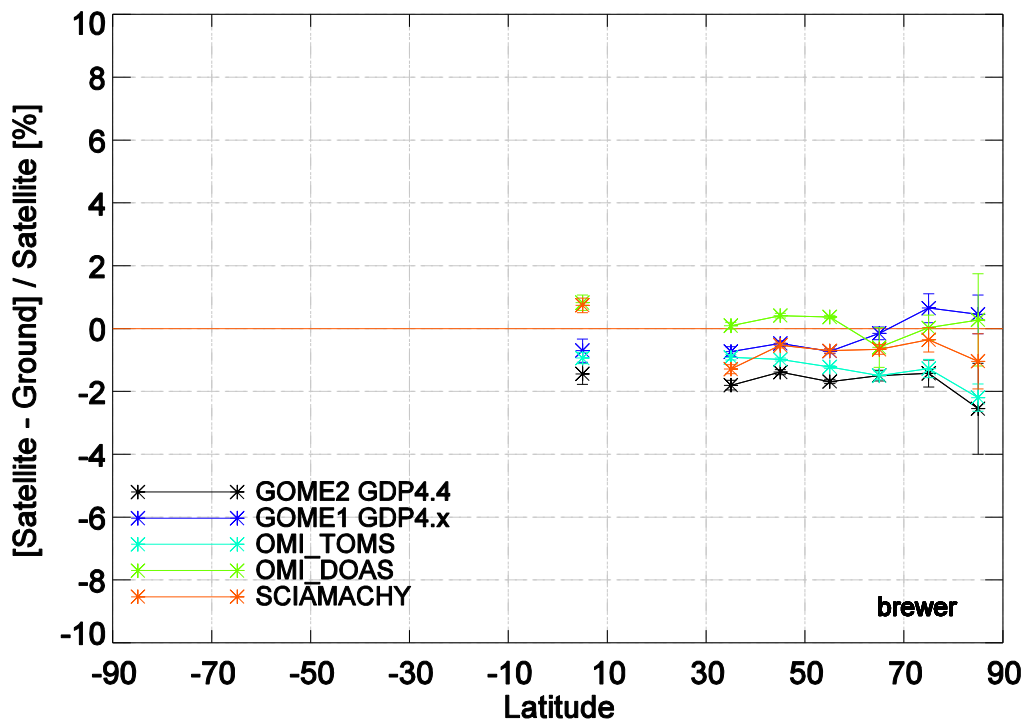
708
709 **Figure 4 First Row, Left.**
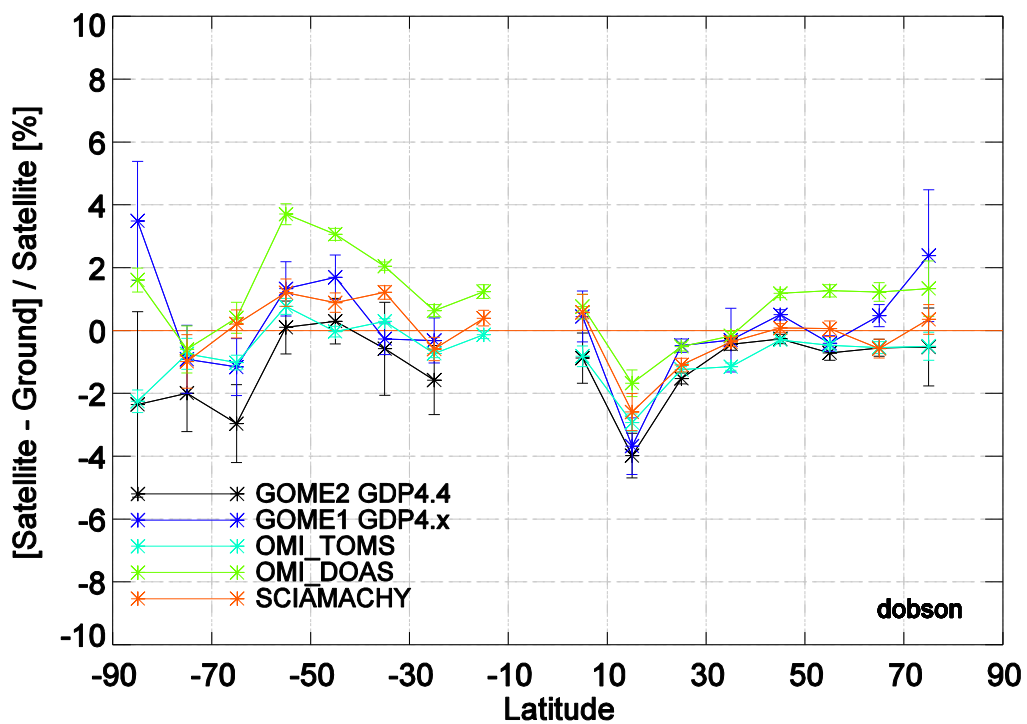
710
711   **Figure 4 First Row, Right.**
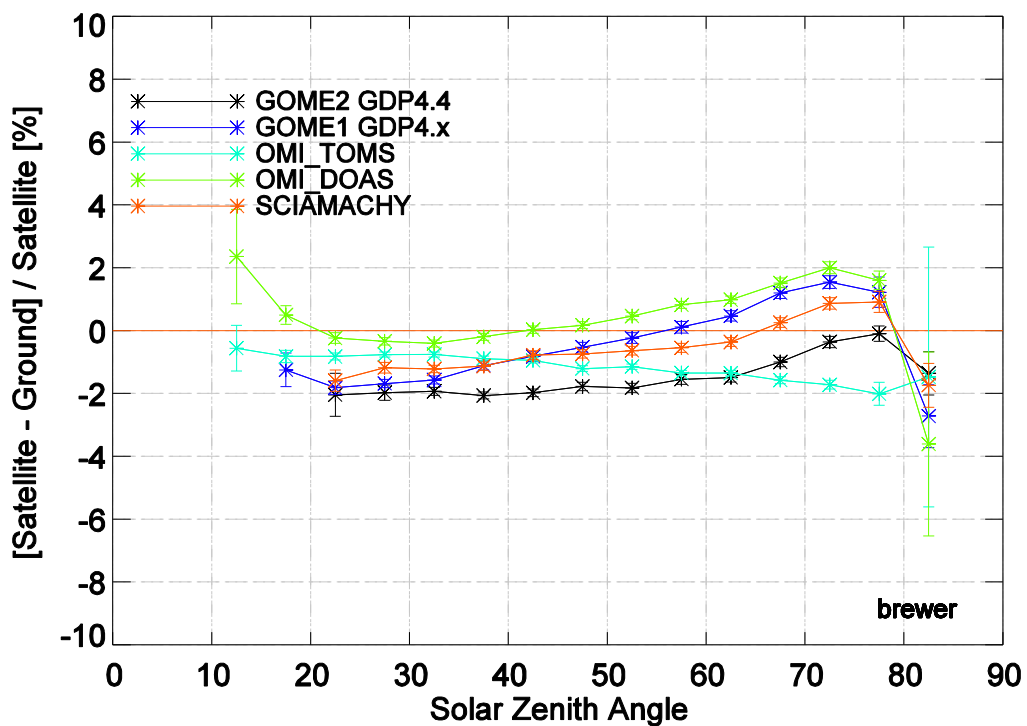
712
713   **Figure 4 Second Row, Left.**
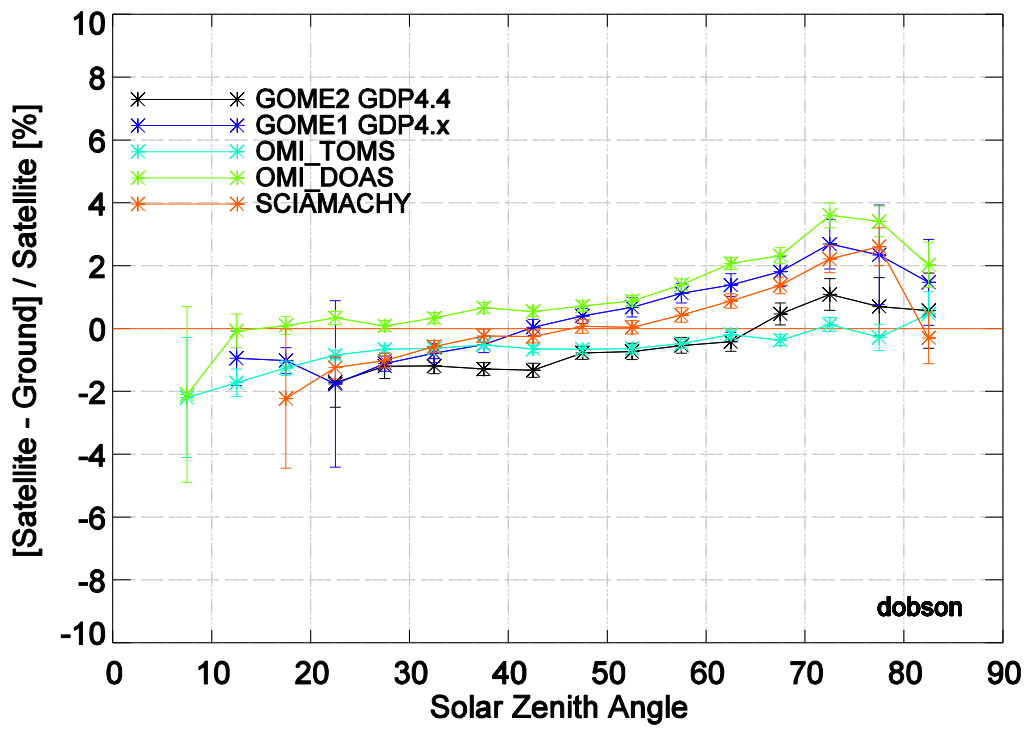
714
715   **Figure 4 Second Row, Right.**
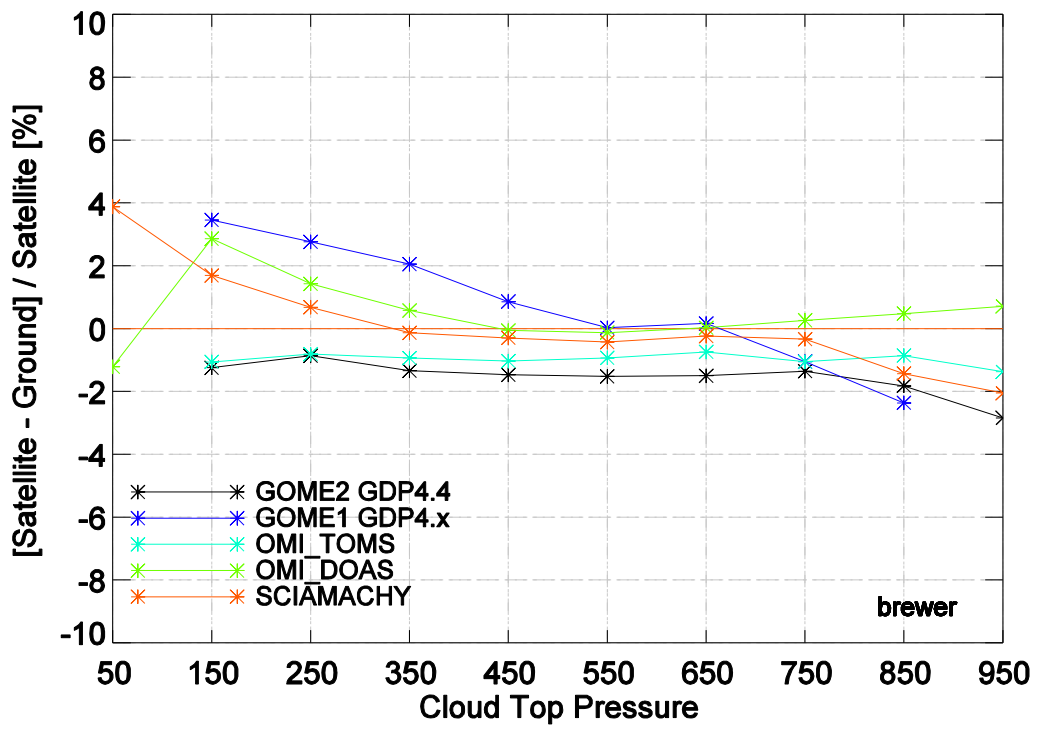
716
717   **Figure 4 Third Row, Left.**
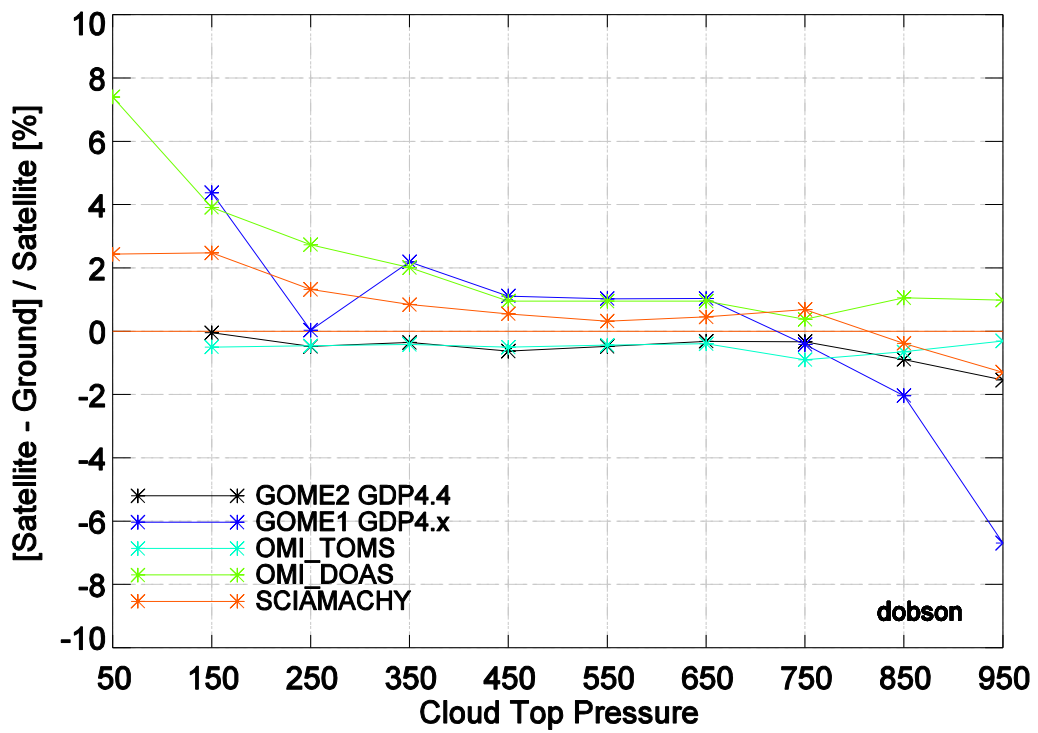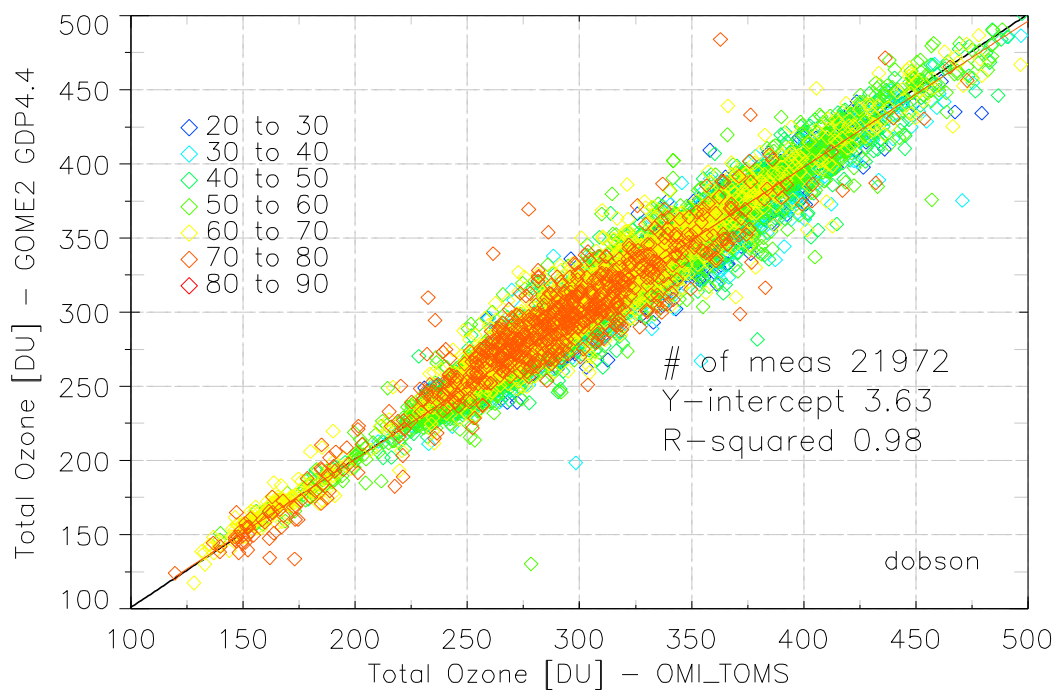
Figure 4 Third Row, Right.
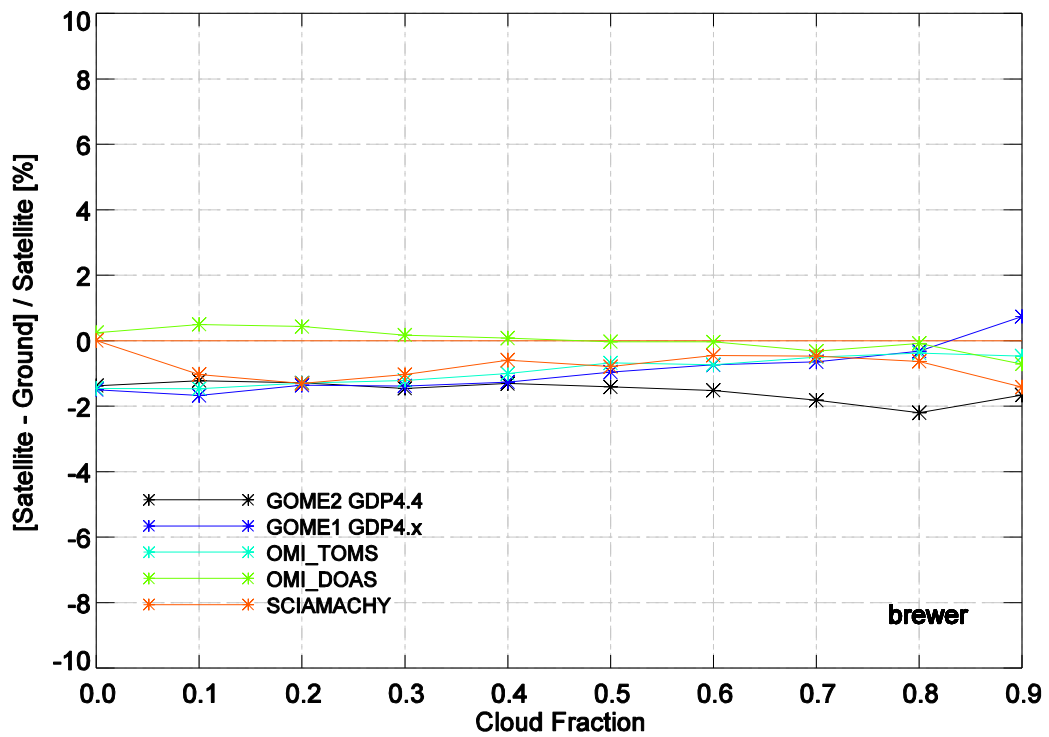
Figure 4 Fourth Row, Left.

722
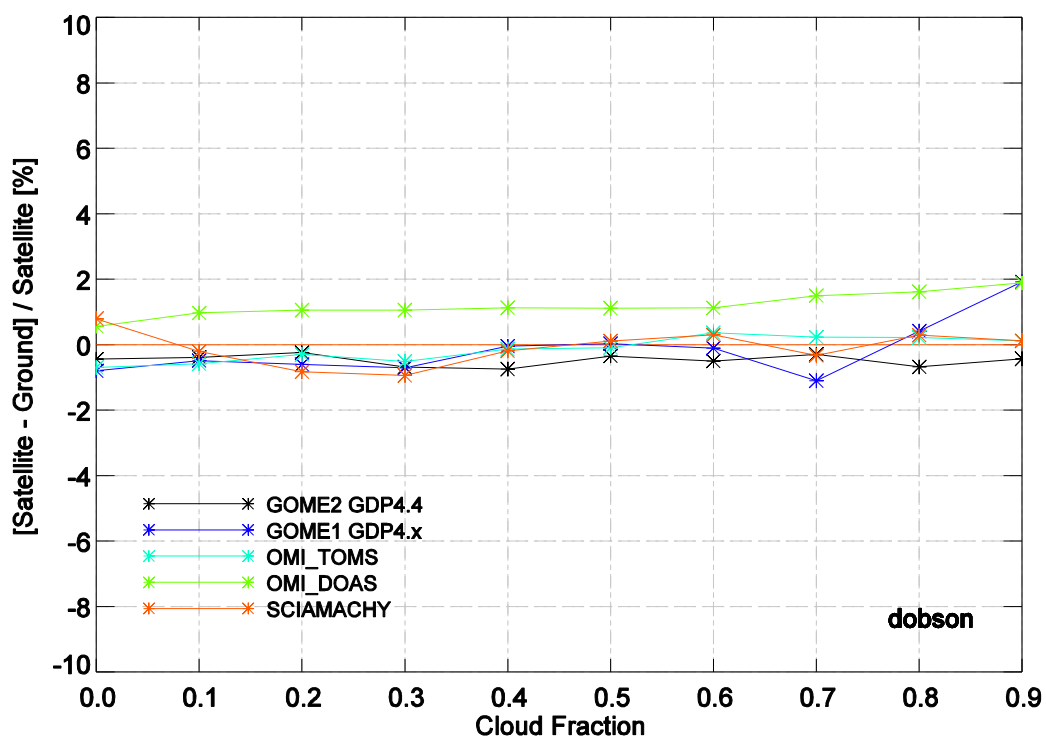
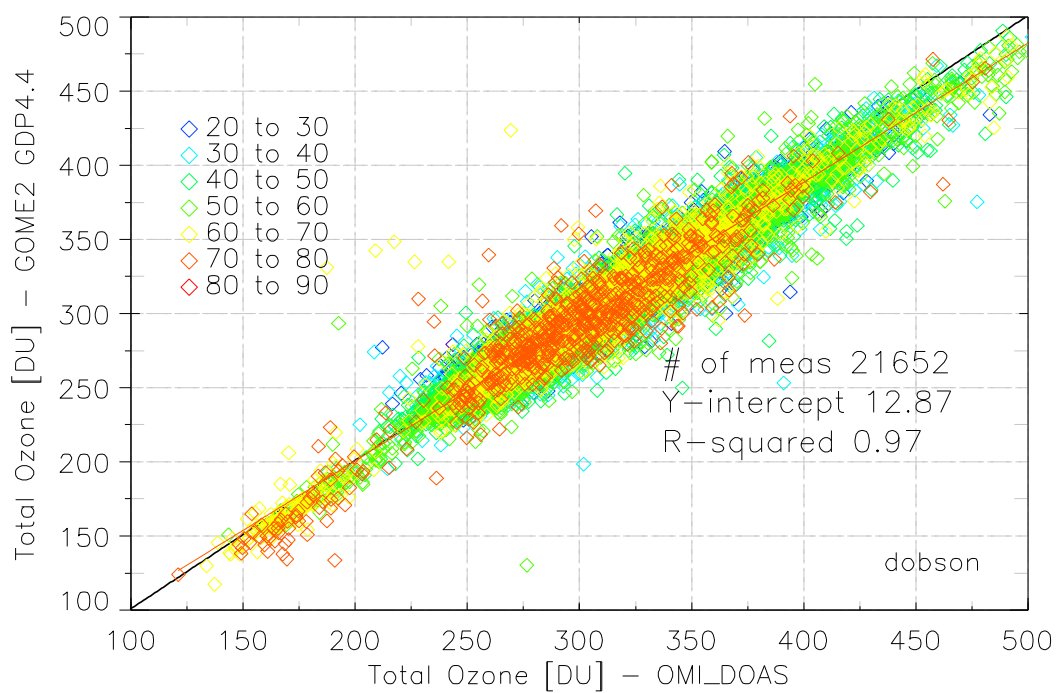724   **Figure 4 Fourth Row, Right.**

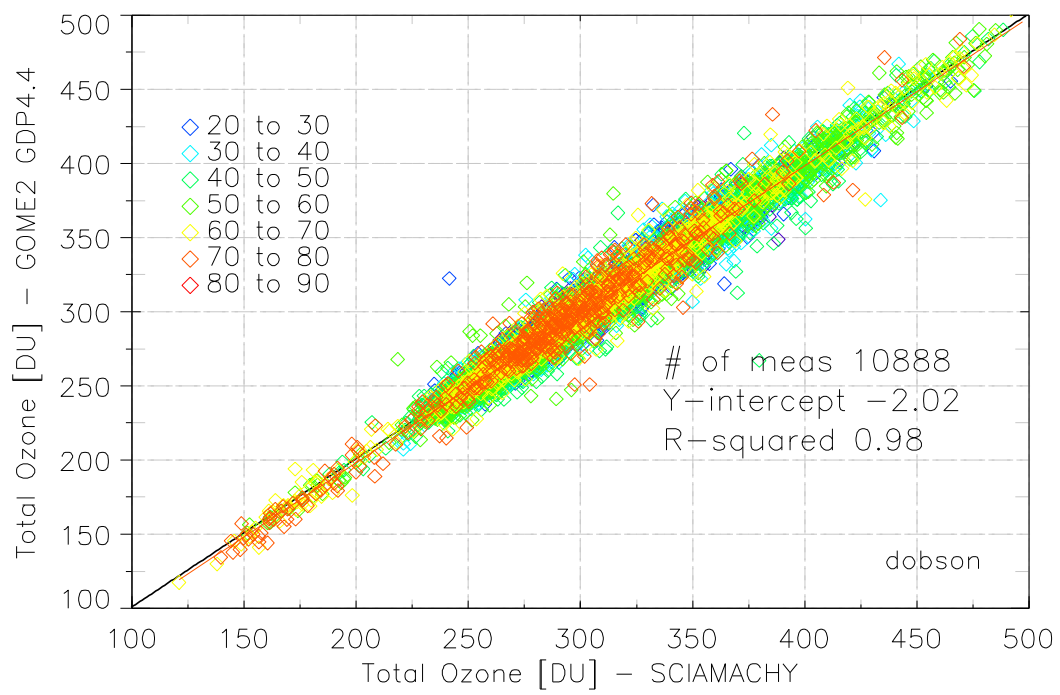**Figure 5 Upper, Left.**
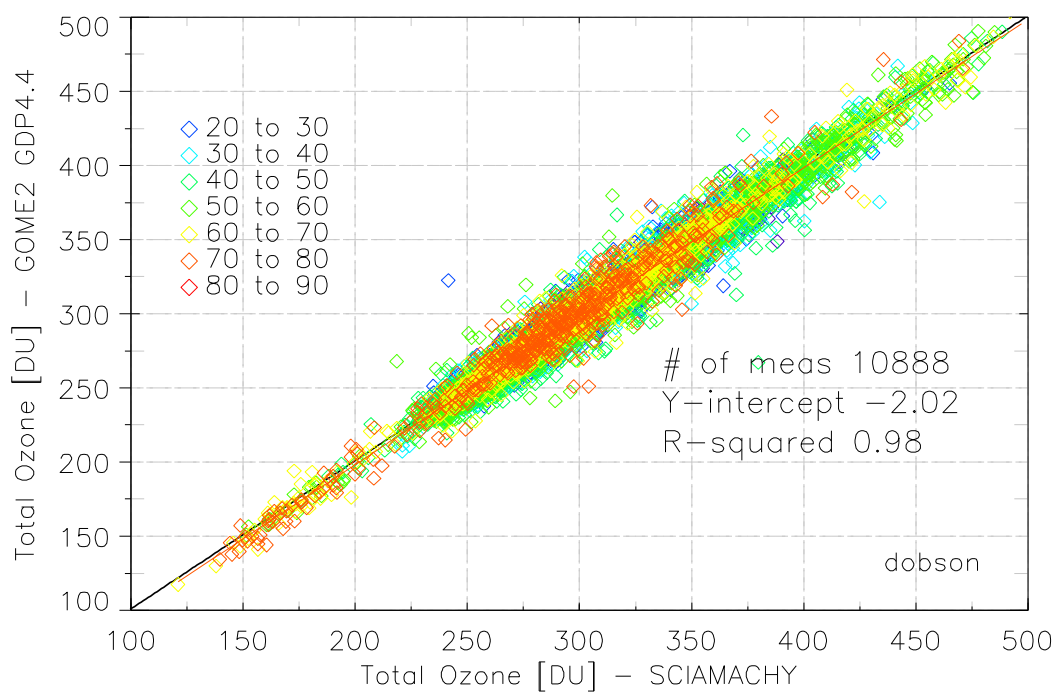
727
728   **Figure 5 Upper, Right.**

729
730   **Figure 5 Bottom, Left.**

731
732

733
734